PYROLYTICALLY SPRAY DEPOSITED ELECTROCHROMIC WO_3 FILMS

by

Zhou Guanghui

B.Sc. (Honours), Hunan Normal University, 1982

THESIS SUBMITTED IN PARTIAL FULFILLMENT OF

THE REQUIREMENTS FOR THE DEGREE OF

MASTER OF SCIENCE

in the Department

of

Physics

SIMON FRASER UNIVERSITY

July, 1987

APPROVAL

Name: Zhou Guanghui

Degree: Master of Science

Title of Thesis: Pyrolytically Spray Deposited Electrochromic WO_3 Films

Examining Committee:

Chairman: L. E. Ballentine

K. Colbow

Senior Supervisor

R. F. Frindt

S. R. Morrison

B. P. Clayman

Examiner
Professor of Physics
Simon Fraser University

Date Approved: 23. July 1987

PARTIAL COPYRIGHT LICENSE

I hereby grant to Simon Fraser University the right to lend my thesis, project or extended essay (the title of which is shown below) to users of the Simon Fraser University Library, and to make partial or single copies only for such users or in response to a request from the library of any other university, or other educational institution, on its own behalf or for one of its users. I further agree that permission for multiple copying of this work for scholarly purposes may be granted by me or the Dean of Graduate Studies. It is understood that copying or publication of this work for financial gain shall not be allowed without my written permission.

Title of Thesis/Project/Extended Essay

Pyrolytically Spray Deposited Electrochromic WO_3 Films

Author:

(signature)

Zhou Guanghui

(name)

August 13, 1987

(date)

ABSTRACT

Pyrolytically spray deposited WO_3 films on various transparent SnO_2:F substrates were investigated by means of X-ray diffraction and the results were correlated to the electrochromic behavior of the films.

The SnO_2:F films with thicknesses greater than 5000A were also pyrolytically spray deposited onto glass slides, using a solution containing stannic chloride and stannous fluoride. The polycrystalline SnO_2:F films, used as the substrate for electrochromic WO_3 films, were highly conducting.

The WO_3 films of thicknesses 400 to 4200Å were deposited onto the SnO_2:F substrates using a tungsten chloride solution. Through X-ray diffraction studies, the deposition parameters (crystallinity of substrate, carrier gas flowrate, substrate temperature during the deposition and deposition time) for controlling the crystallinity and preferential crystallite orientation of the WO_3 films, were qualitatively determined.

The electrochromic performance revealed that polycrystalline WO_3 films with a larger crystallite size and more randomly oriented crystallites showed a larger transmittance change on applied voltage during coloration. These results partially support the hypothesis proposed by Svensson et al.[15], that injected electrons in polycrystalline

WO_3 films with larger crystallite size are likely to show free electron behavior. The effects of the crystallite preferential orientation on the electrochromic behavior of the WO_3 films, were also discussed.

To

my motherland, my Alma Mater and my family.

ACKNOWLEDGMENTS

I wish to express my sincere thanks to my senior supervisor, Dr. K. Colbow, for his encouragement, supervision and financial support throughout this research. Thanks also to Dr. R. F. Frindt and Dr. S. R. Morrison for acting as the members of my supervisor committee and examining committee, and to Dr. B. P. Clayman from the Physics Department for acting as my examiner.

My special thanks go to Dr. S. Wessel, for her concrete guidance and helpful discussions and for her kindness in correcting the hand-written manuscript of my thesis which occupied a great deal of her time. I sincerely thank J. Hickman and D. Craigen for their technical help during the experiments.

Finally, a scholarship from the Chinese Government and the TA'ships from the Physics Department of SFU were also very much appreciated.

TABLE OF CONTENTS

List of Tables

List of Figures

CHAPTER 1

INTRODUCTION

Electrochromism is exhibited by a number of materials, such as transition-metal oxides (WO_3, MoO_3 and V_2O_5). Electrochromism is a reversible color change in a material caused by an applied electric field or current. This change can be due to the formation of color centers (or defect complexes) or to an electrochemical reaction that produces colored compounds [1]. Among these electrochromic materials tungsten trioxide (WO_3) is one of the best examples, and has been widely studied. Since the electrochromic properties of WO_3 thin films were reported by Deb in 1973 [2], many investigations have been carried out on both properties and preparation methods of the film for the purpose of display devices and radiation controlled "smart windows".

Both amorphous and polycrystalline WO_3 thin films show the electrochemical coloration and that the optical properties of the films change during the coloration. Basically amorphous film can be used in display devices because of its fast time response of coloration, and polycrystalline film can be used in windows due to its high infrared reflectance during

coloration [3],[4],[5],[6],[7],[8].

Vacuum evaporated WO_3 films were produced by Fanghnan et al. in 1975 [9]. They constructed some electrochemical cells based on these films to perform electrochemical coloration and proposed a double injection model of positive ions and electrons for the mechanism of WO_3 electrochromism. Miyake et al.[10] carried out systematic measurements of the physical, optical and electrochromic properties of vacuum evaporated WO_3 films in 1983. They concluded that the properties of these films depend considerably on the substrate temperature during the deposition which determines the formation of amorphous or polycrystalline films; films prepared at a substrate temperature higher than 400°C have a resistivity of 10^{-3} to 10 Ωcm and the films prepared at a substrate temperature lower than 350°C were amorphous and transparent with a resistivity of 10^5 to 10^9 Ωcm. Both amorphous and polycrystalline films showed electrochromic behavior [10]. Another method, rf sputtering from a compressed WO_3 target under $Ar-O_2$ atmosphere, was used by Goldner et al. in 1985 [4]. They found that the films prepared at the substrate temperatures higher than 325°C were polycrystalline in structure and showed a high infrared reflection during the coloration. Later, Kaneko et al. [11] investigated a number of properties of the rf sputtered WO_3 films. In addition to the similar results of evaporated films, they found the properties of the rf sputtered films depended on the O_2 concentration and

total pressure of the atmosphere.

Other WO_3 thin film preparation methods, such as electrolytic precipitation, solgel [12] and chemical vapour deposition [13] have been tried recently. A pyrolytic spray deposition technique was reported by Craigen et al in 1986 [14]. In this method WO_3 films were deposited onto a SnO_2:F film substrate by pyrolytically spraying a $WCl_6 \cdot nH_2O$ solution in an open-air atmosphere. They primarily investigated the the structure and electrochromic behavior of the films prepared by this method and found that at a substrate temperature of 400°C, WO_3 deposited onto glass was amorphous, and deposited onto polycrystalline SnO_2:F layer was polycrystalline in structure itself. They also reported that WO_3 films prepared by this method showed similar electrochemical coloration to the WO_3 films prepared by other methods. Comparatively this method is simple and inexpensive, and has the potential to produce large area electrochromic coatings with low capital and production costs.

Coated window glass is being used on an increasing scale for gaining energy efficiency. Essentially, if the onset of high reflectance of the coatings occurs at a wavelength of about 0.7 μm, such coatings can be used for decreasing the inflow of infrared solar radiation therefore diminishing the need for air conditioning in a warm climate. If the onset of the high reflectance is instead at a wavelength of about 3.0 μm, the coatings provide low thermal isolation desired in a

cold climate. Many authors [4], [7], [15], [16] proved that electrochemically double injected polycrystalline WO_3 films show a metallic, i.e. an approximate free-electron behavior resulting in a high adjustable infrared reflection with different density of injected electrons and satisfy the above condition. Based on the double injection model, Svensson et al. computed the visible and infrared reflectance of ideal crystalline WO_3 films as function of electron density . Their theoretical result give twice the experimental value of reflectance for an rf sputtered polycrystalline WO_3 film in a deeply colored state reported by Goldner et al. [4]. This discrepancy was interpreted by Svensson et al.[15] as a poor crystallinity of the film, which produces grain boundaries, neutral defects, dislocations, etc.

AIMS AND STRUCTURE

The aim of this thesis is to investigate the pyrolytic spray deposition parameters for controlling the degree of the crystallinity, such as crystallite size and preferential orientation of the WO_3 films, and the correlation between crystallinity and electrochromic behavior of the WO_3 films.

Chapter 2 describes the basic considerations of an electrochromic cell. WO_3 crystal structure, the structure of WO_3 in the form of thin films and the models of

electrochromism are discussed. A computation of theoretical reflectance modulation of polycrystalline WO_3 film is also introduced.

Pyrolytic spray deposition apparatus and materials as well as experimental methods are described in chapter 3.

Chapter 4 presents the results of this research and gives a detailed discussion of the deposition parameters for controlling the degree of the crystallinity of the WO_3 films. The electrochromic behavior of the WO_3 films is explained in relation to their crystallinity. The conclusion follows in chapter 5.

CHAPTER 2

WO_3 THIN FILMS AND ELECTROCHROMIC CELL

2.1 ELECTROCHROMIC CELL

Fig.2.1 shows the sandwich structure of a typical electrochromic cell (ECC) [5], [6]. Generally, an ECC operates between two electrode layers. These can be semi-transparent metals, such as a 50 to 100Å thick gold film or transparent doped simiconductor layers, such as indium-tin-oxide (ITO) or F doped tin oxide films. For the purpose of larger area window shutter, the two electrode layers should be as transparent as possible in the visible region of the solar spectrum and highly conductive. It is important to keep the electrical resistance of the electrodes as low as possible to minimize current loss and heating of the window [18]. In both liquid and solid electrolyte cells, it is important that the electrolyte or fast-ion conductor should not react chemically with the electrodes. The ions needed in the electrochromic reaction are provided by the ion storage and are injected in the coloration process into, or withdrawn in the bleaching process from , the electrochromic layer through the ion

conductor. The electrons needed in the coloration process are provided by the electrochromic substrate layer. For cells using liquid electrolytes , the electrolyte can serve as both storage and conductor for ions. While in all-solid-state cells the ion conductor can be an appropriate dielectric and the ion storage can be another electrochromic layer (preferably anodic if the base electrochromic layer is cathodic, or vice versa). One may also combine the conductor and storage media into one layer [6]. The electrochromic layer which has been widely studied is a WO_3 thin film because of its appropriate characteristics. Other inorganic partially hydrated transition metal oxides such as MoO_3 [19] and organic substances such as $C_{10}H_8N_2$ [18], also have been tried.

The optical properties of ECC for windows are continuously switchable between colored and bleached states. The nature of this switching can be different depending on the basic requirement on the cell, i.e. whether the main goal is to achieve control of the energy flowing through the window, or if daylighting and glare control are of prime importance. Under certain conditions, it may also be possible to have variable thermal insulation.

There are two general approaches to achieving variable transmittance: modulation of absorptivity or of reflectivity. Either form of the modulation would result in benefits of thermal stability of interior space. However,

reflection modulation is highly desired for window purposes. The optical properties of the polycrystalline WO_3 film are conveniently treated in terms of modulated reflection because the injected electrons exhibit an approximately free-electron behavior, whereas amorphous WO_3 films are treated in terms of modulated absorption because the injected electrons are highly localized in W^{+5} sites [6], [9], [16], [18].

2.2 THE PHYSICAL PROPERTIES OF WO_3 FILMS

The structure exhibited by a material in the form of a thin film depends on the film preparation conditions. For the WO_3 thin film prepared by the methods described in the introduction, the substrate temperature, the crystallinity of of substrate , the pressure of the atmosphere and the carrier gas flowrate are important parameters. Especially, the substrate temperature can result in an amorphous or polycrystalline structure of the films prepared. Both uncolored amorphous and uncolored polycrystalline films are transparent. In visible and infrared regions the refractive index is about 2.2 [2], [10], [11], [20], and the extinction coefficient before coloration is about 0.1 which results in small absorption before coloration [20]. During coloration, the optical density of electrically colored amorphous films increases about 7 times and for polycrystalline films the

optical density increases only 2 times in the near infrared region (1.5eV) [16]. X-ray diffraction and electron microscope observations revealed that the films prepared by the methods described above are composed of a tungsten mixed oxide with the composition of $WO_{2.83}$, $W_{20}O_{58}$ and WO_3, and are mainly WO_3 in composition [2], [4], [10], [14].

Since Brakken found that WO_3 has perovskite-like structure [22], many authors have investigated WO_3 with a view to understanding its physical properties [17], [23], [24], [25], [26], [27], [28], [29]. On the basis of the cubic approximation of the WO_3 lattice, Kopp et al. calculated the the energy band structure of WO_3 using the Green's function method [23]. The calculated band gaps were about 50% smaller than the optical measured values of about 2.6 eV for the indirect gap and 3.5 eV for the direct gap reported by Koffyberg et al. [24].

WO_3 single crystals are thought to exhibit at least five phases in the temperature range from 900 to -180°C, changing through the sequences tetragonal, orthorhombic, monoclinic, triclinic and monoclinic during cooling [17], [25]. Salje found that WO_3 exhibits orthorhombic symmetry with the unit cell dimensions of a=7.341Å, b=7.570Å and c=7.754Å in the temperature range from 467 to 680°C [28]. Tanisaki found WO_3 to be of monoclinic symmetry with unit cell parameters of a=7.30Å, b=7.53Å ,c=7.68Å and β=90.54° at room temperature [25], but the $\vec{c}$ axis length is twice that

reported by others [30]. WO_3 thin films prepared at substrate temperature from 350 to 500°C were found to be the mixture of monoclinic, triclinic and orthorhombic in structure [10], [14]. However, these types of structure are perovskite-like based on the corner-sharing and packing of WO_6 octahedra as shown in Fig.2.2 [17]. The structure analyses of WO_3 have revealed considerable deviations from the ideal cubic perovskite type. For the orthorhombic symmetry, the deviation from the ideal perovskite structure is characterized by a zigzag displacement of the W atom in the $\vec{b}$ and $\vec{c}$ crystallographic directions as well as a tilt system with tilt angles around the $\vec{a}$ crystallographic direction [28]. On the other hand, the distortions of the monoclinic structure correspond to displacements of W atoms and mutual rotations of the oxygen octahedra. As shown in Fig.2.3, the W-O bonds of the monoclinic structure form zigzag chains along the three crystallographic axes, with W-O-W angles of 158±2.3° and O-W-O angles of 166±5.6°. In the $\vec{a}$ crystallographic direction the W-O bonds are of roughly equal length (1.9Å), while in the $\vec{b}$ and $\vec{c}$ crystallographic directions the W-O bonds are alternately long and short (2.1Å and 1.75Å respectively). As in most perovskite-like structure substances, the magnitude of the above deviations from the cubic symmetry depend on temperature [17].

The structure of amorphous WO_3 in the form of thin films has also been widely investigated [8], [29]. It is composed

of a spatial oxygen network of tightly bound $(WO_6)_n mH_2O$ clusters with a large number of terminal oxygen W=O and W-O-W bonds between clusters. Using Raman scattering, Gabrusenoks et al.[29] found that the clusters with dimensions not larger than 20 to 30Å (to preserve X-ray amorphousness) are linked together in such a manner as to guarantee a porous structure of the amorphous WO_3 films. The clusters in the amorphous WO_3 films contain at least two types of WO_6-octahedra: one with a oxygen terminal and one without it, which represents an axially distorted and a generally distorted octahedron, respectively [29].

The crystal structure of tungsten bronze has been studied extensively [18], [30], [31]. By the injection of different cations, one can form different tungsten bronzes such as Li_xWO_3, Na_xWO_3, K_xWO_3 and H_xWO_3 [18], where generally $0<x<3$. Wiseman et al. used a deuterium analogue to determine the structure of H_xWO_3 [31]. From neutron diffraction studies the authors concluded that the crystal structure of H_xWO_3 has a similar structural progression from distorted WO_3 to the cubic perovskite type structure at high x value. The W atoms are arranged on a simple cubic lattice and are surrounded by almost regular octahedra of O atoms linked together by corner sharing. The octahedra are tilted 11° and form the W-W direction, producing an O-O distance between adjunct octahedra of 3.264Å. Statistically the deuterium atoms are attached to all O atoms with a bond length of 1.1Å long

and a displacement of 11.8Å off the stright line to the neighbouring O atom. The deviation from a normal O-H bond length (1.0Å) may be significant since it is quite feasible that the O atoms are relaxed from their average positions whenever a deuterium atom is attached. So by analogy the atoms in H_xWO_3 form an OH bond with one of its surrounding O^{-2} neighbors, so that the chemical formula of the hydrogen bronze should be $(OH)_xWO_{3-x}$. In the limiting case of x=3, a tungsten hydroxide $W(OH)_3$ would result and the "hydrogen tungsten bronze structure" was indeed found for the trivalent hydroxides $In(OH)_3$ and $Sc(OH)_3$ [31].

2.3 ELECTROCHROMISM OF WO_3 FILMS

Many investigations have been carried out in the effect to understand the electrochromism of WO_3 films. Until about 1975 it was believed that a current applied to WO_3 produced a redox reaction to form a blue-colored oxide product . The reaction was proposed to be [32]:

$$xWO_3 + 2yH^+ + 2ye^- \longrightarrow W_xO_{3x-y} + yH_2O \qquad (2.1)$$

A similar model for this system was suggested at same time by Hurditch et al. [33], which dicusses the formation of a complex of WO_x^+ and OH^-, i.e. the extraction of oxygen

according to the following reaction:

$$WO_3 + yH^+ + ye^- \longrightarrow WO_{3-y}(OH)_y \qquad (2.2)$$

Another model proposed by Faughnan [9] fits most experimental data [34]. It involves intervalence transition absorption for electrocoloration of WO_3. Coloration of the film was achieved by simultaneous injection of cations and electrons into interstitial sites in the WO_3 atomic lattice, forming a tungsten bronze, according to the following equation :

$$WO_3 + xM^+ + xe^- \longrightarrow M_xWO_3 \qquad (2.3)$$

where M is a positive ion, in the simplest case a proton, H^+. In amorphous films this model accounted for coloration by intervalence transfer absorption [8], stated as:

$$W^{5+}(A) + W^{6+}(B) + h\nu \longrightarrow W^{6+}(A) + W^{5+}(B) \qquad (2.4)$$

where A and B are two different lattice sites. Another model closely related to Faughnam's theory suggests that the presents of a polaron, which is an electron loosely bound to its accompanying lattice distortion, causes coloration of the WO_3 films [16]. In both models coloration is attributed to the tight localization of conduction band electrons to W^{5+} sites.

The W^{5+} species form a defect band that is localized within the WO_3 bandgap. However, coloration could also be explained by delocalized electrons and free electron plasma absorption [18]. This effect has been ruled out because in amorphous films a broad absorption peak is noted over the range of 1.2 eV to 1.5 eV, rather than the sharp peak characteristic of a plasma [16].

Some of the experimental results supported the double injection model. Nishimura et al. [35] measured the infrared absorption spectra of WO_3 cells at coloration, they observed a rather strong absorption at shorter wavelength and ascribed the peak to W^{5+}, which peaks at approximately 1.0μm. A weak but clear absorption peak at 4.3 μm is observed only in the colored samples, which can be ascribed to the O-H stretching vibration [35]. Dickens et al. studied the enthalpy changes for hydrogen insertion into WO_3 film by using solution calorimetry [36]. The results supported the double injection model. Schirmer et al.[16] pointed out that since all tungsten sites are not equivalent in an amorphous material, the injected electrons will be preferentially trapped at deeper sites. This variation in trap depths will add an additional term E_o to the energy of the transition. This is supported by the fact that the optical absorption shifts to lower energy in crystalline WO_3 films [16]. Crandall et al.[37] measured the variation of the chemical potential (μ_H) of hydrogen in amorphous films of H_xWO_3 and reported that as the coloration

proceeds an internal electromotive force appears which is a function of the stoichiometric parameter x value in H_xWO_3.

Some of the experimental results could not be explained by the double injection model, for instance, coloration under UV illumination and annealing in a vacuum without hydrogen (or cation) injection [2]. Muramatsu et al. [38] compared SIMS (Secondary Ion Mass Spectroscopy) results of electrochemically colored and bleached WO_3 films and found that the spectra peak heights of hydrogen atoms were the same in both cases, and the OH^- and H_2O contents were also the same in both cases. In addition, they compared the XPS (X-ray Photoelectron Spectroscopy) results of WO_3 films colored and bleached by the same method and showed that the stoichiometry of the films from the peak height ratio of oxygen to tungsten were the same in both cases, and there was no extraction of oxygen from the WO_3 during the coloration at least at the surface of the film [37]. Recent electron resonance studies argued against both intervalence transfer and small polaron models [38]. In this point electrons are not uniquely localized in H_xWO_3 in either amorphous or polycrystalline films. If W^{5+} is formed during coloration, the donated electrons must be delocalized over a number of tungsten sites [16]. In the fine grained polycrystlline film a model was proposed by Dautrement-Smith et al.[39] which follows the double injection model with consideration of localized electrons in deep donors in grain boundaries [39]. Although the

understanding of the mechanism of the coloration of WO_3 films is not completed now, the double injection and intervalence transfer model which was first proposed by Faughnam et al.[9] seems the most reasonable explanation and is widely accepted.

2.4 REFLECTION MODULATION OF WO_3 FILM

On the basis of the double injection theory, the theoretical reflectance of polycrystalline WO_3 film was first computed by Svensson et al. [6], [7]. Introduction of electrons and positive ions into the WO_3 film gives an electron density N_E and an equal density of ions N_I. Electrons with N_E in excess of the Mott critical density [40] are assumed to occupy the WO_3 conduction band in the form of an electron gas. Damping of the free electrons occurs, in principle, from scattering by ionized impurities, neutral point defects, dislocations, crystallite boundaries etc. For a sufficiently ideal film one may neglect all but the ionized impurities — an unavoidable consequence of the double injection model [7], [9]. The dielectric function can be written as [5]:

$$\varepsilon = \varepsilon^{WO_3} + \frac{i}{\varepsilon_0 w_p \rho} \qquad (2.5)$$

with

$$\rho = i\frac{Z^2N_I}{6\pi^2\varepsilon_o N_E^2 w}\int_o^\infty k^2dk\left[\frac{1}{\varepsilon^L(k,w)} - \frac{1}{\varepsilon^L(k,0)}\right] - i\frac{w}{\varepsilon_o w_p^2} \qquad (2.6)$$

Here ε^{WO_3} is the dielectric constant of the WO_3 host lattice, $\hbar w$ is the photon energy, ε_o is the permittivity of free space, $\rho = \rho_1 + i\rho_2$ is the complex dynamical resistivity of the damped electron gas, and Z is the charge of the point-like defects, which are screened by a dielectric function ε^L. ε^L is dependent on wavevector k and frequency w, and can be given by the random phase approximation [41]. w_p denotes the plasma frequency.

Fig. 2.4 illustrates the reflectance at normal incidence of a 2000Å thick crystalline WO_3 film with electron density N_E from 10^{21} to $10^{22}/cm^3$ computed by Svensson et al. according to equations (2.5) and (2.6). In Fig.2.4 the dashed curve represents the reflectance of an rf sputtered polycrystalline WO_3 film with high densities of H^+ and e^- state as measured by Goldner et al. [4]. Cogan et al. reported the reflectance of this film with injected Li ions [42], and obtained the similar result as Goldner et al.[4]. The experimental values were lower than the theoretical computed

values. This difference was interpreted by some researchers [4], [6], [7] as being caused by the assumption of ideal ionized scattering. The actual film is of polycrystalline structure and the crystallinity, such as crystallite size and morphology may affect the electron scattering mechanism and the electrochromic behavior of the films.

Fig.2.1 The sandwich structure of an electrochromic cell.

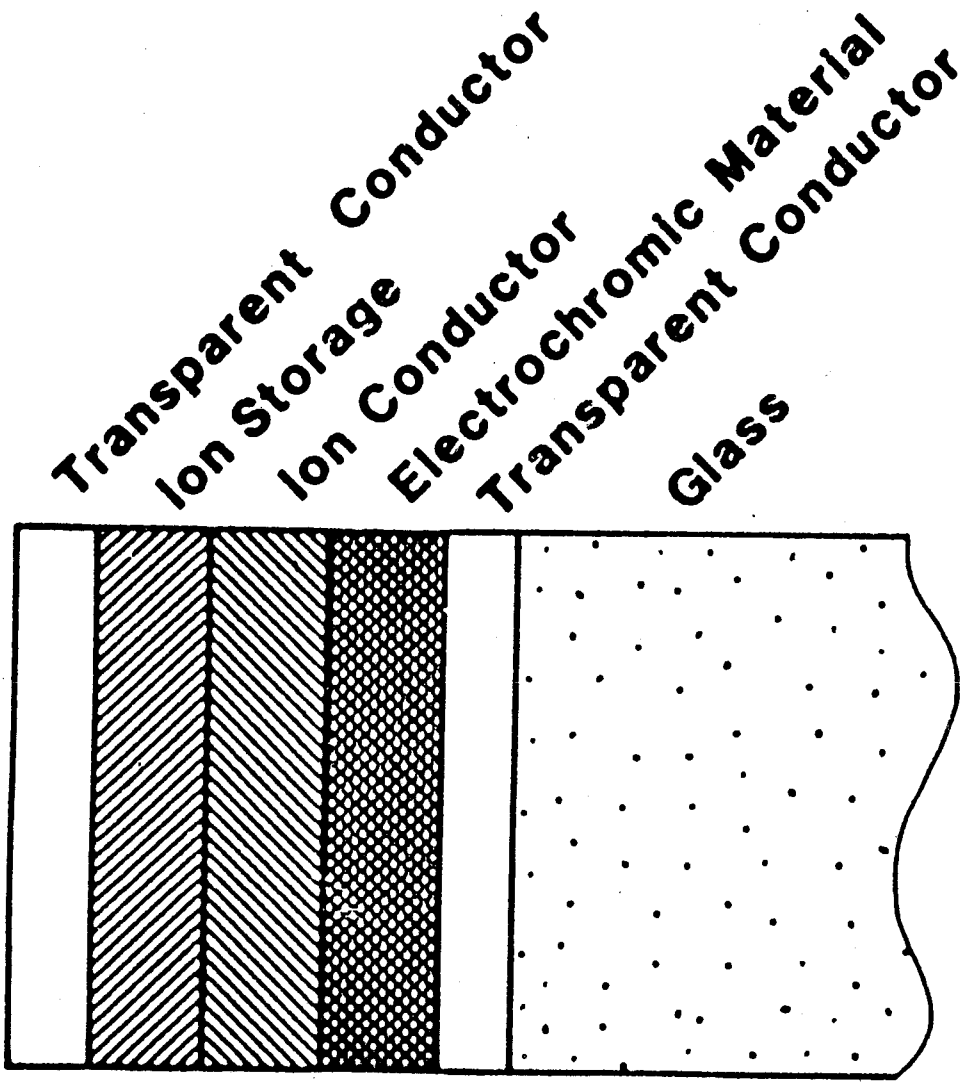
Transparent Conductor
Ion Storage
Ion Conductor
Electrochromic Material
Transparent Conductor
Glass

Fig.2.2 The oxygen octahedron packing of the WO_3 crystal structure

● : W atoms

○ : O atoms

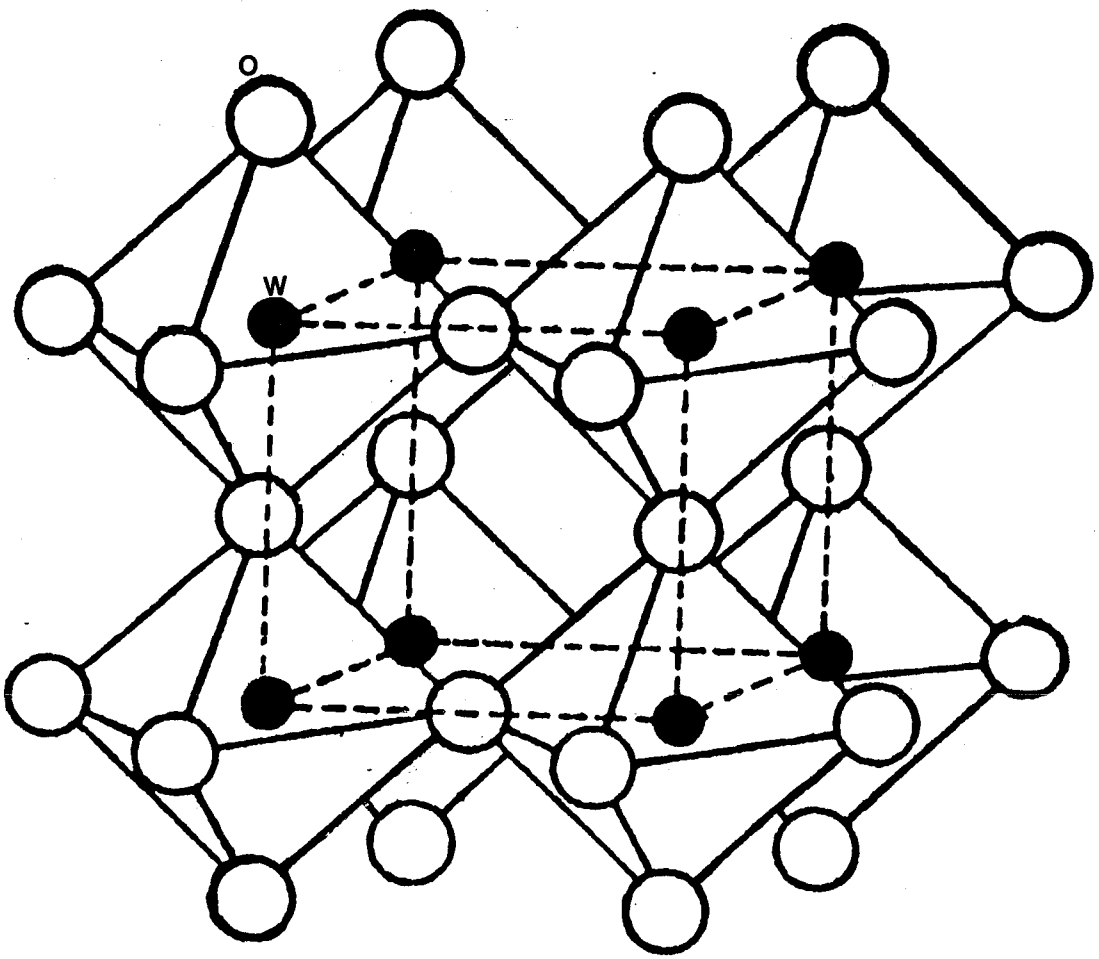
O
W

Fig.2.3 The monoclinic WO_3 structure showing the distorted WO_6 octahedra projected along the y axis.

Only W atoms between y±0.3b are shown; atoms at y≈0 are solid, atoms at y≈+1/4b are dashed, those at y≈-1/4b are dotted [17].

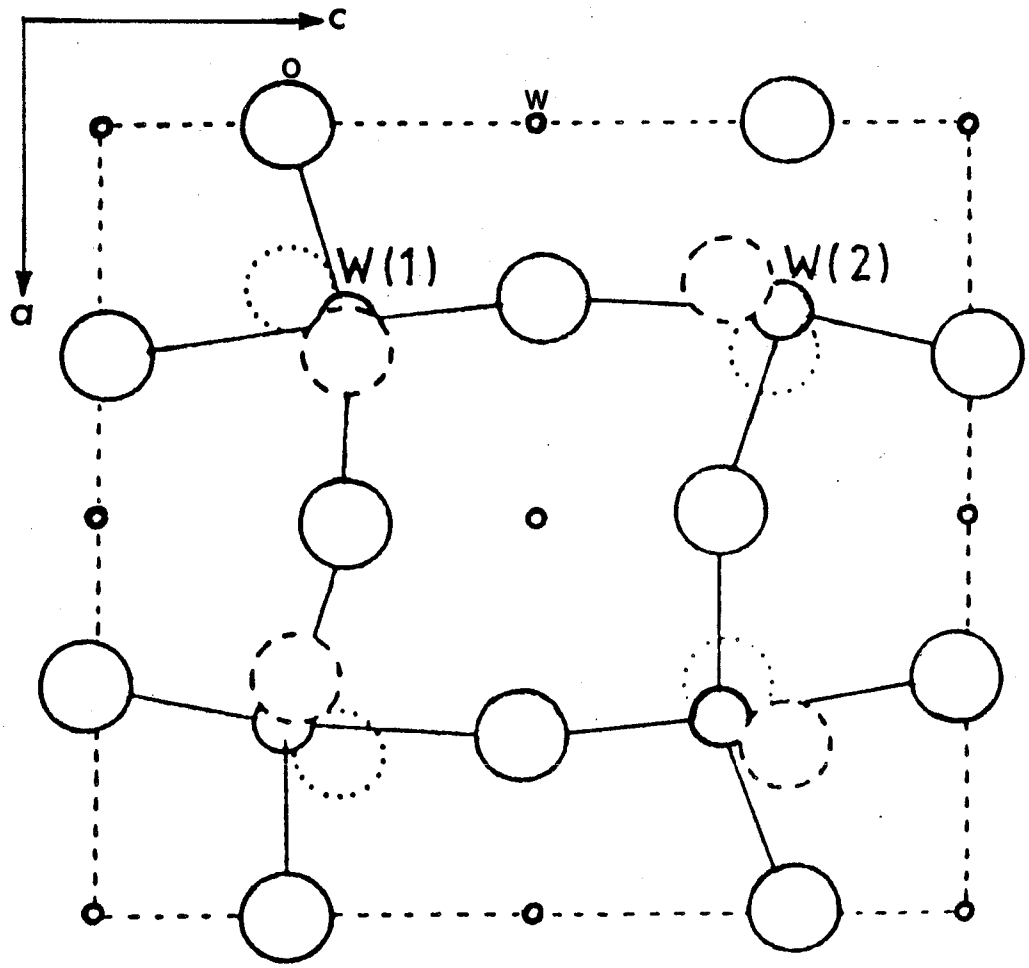
c
a
O
W
W(1)
W(2)

Fig.2.4 Reflectance spectra computed for the configuration given in the inset.

The electrochromic WO_3 layer has the shown magnitudes of electron density N_E. The shaded area denotes the luminous efficiency of the eye and the thin curve represents a typical solar irradiance spectrum. The dashed curve represents the reflectance measured by Goldner et al. [4],[17].

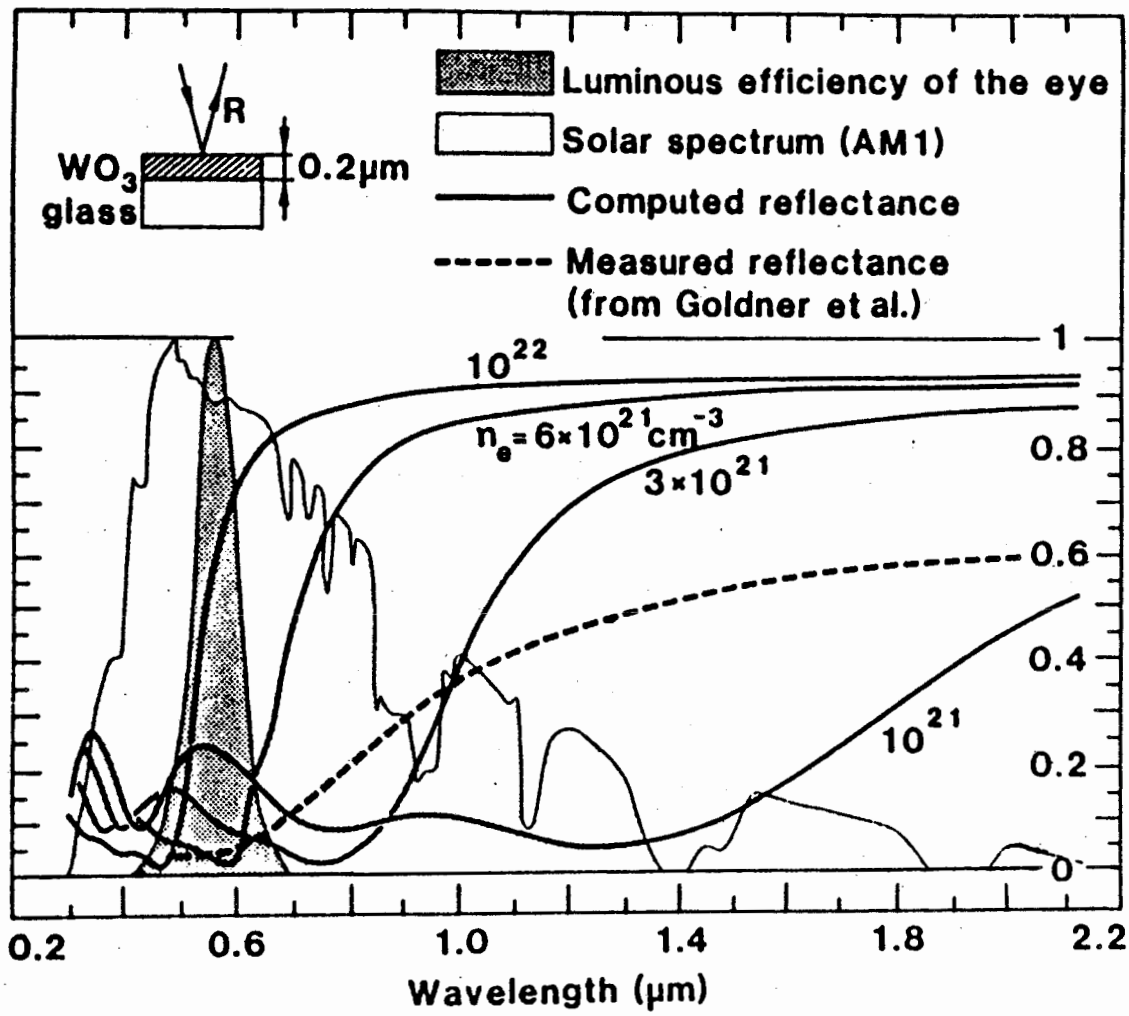
R
WO_3
glass
0.2μm
Luminous efficiency of the eye
Solar spectrum (AM1)
Computed reflectance
Measured reflectance
(from Goldner et al.)
10^{22}
$n_e = 6\times10^{21}cm^{-3}$
3×10^{21}
10^{21}
1
0.8
0.6
0.4
0.2
0
0.2
0.6
1.0
1.4
1.8
2.2
Wavelength (μm)

CHAPTER 3

MATERIALS AND METHODS

3.1 PREPARATION OF SnO_2:F FILM SUBSTRATE

The method of preparation of SnO_2:F films is exactly the same as that used for WO_3 films and will be described in detail later. 20 SnO_2:F films (substrate: 7.5X2.5 cm^2 microscope glass slides) were prepared at a time.

For each type of SnO_2:F substrate, 30 grams of hydrated stannic chloride powder ($SnCl_4 \cdot 5H_2O$, 97.5%, BDH Chemical Ltd.) and 2.4 grams of stannous fluoride powder (SnF_2, BDH Chemical Ltd.) were dissolved in distilled water to produce 80 ml solution. This solution was then sprayed using an ultrasonic nebulizer, which was designed and assembled in our laboratory.

Pyrolysis of $SnCl_4$ is the basic reaction involved in the process:

$$SnCl_4 + 2H_2O \text{ -- } SnO_2 + 4HCl \qquad (3.1)$$

The substrate temperature was controlled between 300 °C

and 500 °C to obtain different types of substrates for the WO_3 films. The spray time was sufficiently long to make films thick enough to eliminate the size effect on electrical conductivity of SnO_2:F films.

3.2 APPARATUS AND PROCEDURES OF PYROLYTIC SPRAY DEPOSITION

For each WO_3 film sample, 3 grams of WCl_6 powder (Johnson Matthey Inc.) were weighed using a triple beam balance in a dry box. The powder was then dissolved in 50 mls of N-Dimethyl formamide ($CON(CH_3)_2$, 98.415%, BDH Chemical Ltd.) solution. The solution which was dark red in color was then immediately sprayed.

The chemical reaction may be written as :

$$WCl_6 + 3/2O_2 \longrightarrow WO_3 + 3Cl_2\uparrow \qquad (3.2)$$

Fig.3.1 shows the design of the pyrolytic spray deposition oven which was built in our lab. An EN 145 electronic nebulizer (Medigas Pacific Ltd., Burnaby, B.C.) was used as the aerosol generator. The spray tube was a stainless steel cylinder with a 16x0.3 cm^2 spraying slit. The distance between spraying slit and the electric heater was about 3 cm, and the angle of the slit with respect to the film substrate was about 45°. A 3PN116 powerstat variable transformer was used to supply

power for the electric heater. The temperature of the electric heater was varied by changing the voltage of the transformer. The spray tube and the electric heater were contained in a wooden box with a glass window through which the substrates and the WO_3 samples can be taken in and out respectively. N_2 was passed through an airflow meter and used as the carrier gas.

Prior to spraying, the heater with tin bath was heated to the required temperature which was measured using an infrared galvanic detector. The SnO_2:F substrate was then placed on the heater for 20 minutes heating prior to spraying. The tin bath served as thermal contact between heater and substrate to be sprayed.

3.3 X-RAY DIFFRACTION STUDIES

The X-ray diffraction experiments were carried out using a computerized diffractometer with CuKα line radiation. The diffraction patterns were compared with the results of published literature [9], [43] and the diffraction peaks were predicted by

$$\frac{1}{d^2} = \frac{i^2}{a^2} + \frac{j^2}{b^2} + \frac{k^2}{c^2} \qquad (3.3)$$

and the Bragg condition

$$\lambda = 2d \sin\theta \qquad (3.4)$$

The average crystallite size t of WO_3 films was calculated by the Scherrer formula [44]

$$t = \frac{0.9\lambda}{B\cos\theta} \qquad (3.5)$$

where

$$B^2 = B_M^2 - B_S^2 \qquad (3.6)$$

and θ is the diffraction angle, B_M is the broadening (radians) of the diffraction peak measured at half its maximum intensity. There are two factors contributing the broadening B_M: one is the instrumental broadening B_S (0.2°) and the other is pure diffraction broadening B when the crystallite size of the film is less than about 1000Å (0.1 μm). Pure diffraction broadening increases with decreasing crystallite size and at sizes less than 100Å the back-reflection peaks disappear entirely and the low-angles peaks become very wide and more diffused [44].

It was worth noting that the crystallite size calculated by this method leads to a determination of the average crystallite size only.

In order to check the structure of the pyrolytically spray deposited WO_3 films, X-ray diffraction

measurements were carried out on a few samples of the tungsten chloride solution sprayed onto glass slides, H_2WO_4 powder heated in the pyrolytic spray deposition oven for a few hours and pure untreated H_2WO_4 powder (98%, BDH Chemical Ltd.). The chemical reaction of heating H_2WO_4 is thought to be:

$$H_2WO_4 \longrightarrow WO_3 + H_2O \qquad (3.7)$$

By comparing the diffraction patterns of the tungsten chloride solution sprayed onto glass slide with the heated H_2WO_4 powder we can identify the characteristic diffraction peaks of the pyrolytically spray deposited tungsten trioxide films.

3.4 MEASUREMENT OF FILM THICKNESS

The thicknesses of the SnO_2:F and WO_3 films were measured by an interference step method using a microscope with an interferometer attachment (Wild Heebrugg Ltd., Switzerland). A hole step was made on the sample by placing a small amount of Zn powder on the film and adding a small amount of concentrated HCl acid. After the reaction the film was rinsed from with distilled water. A few films were re-measured using a mechanical " taly-step " technique (Taylor-Hobson, Model 3) and approximately the same results were obtained.

3.5 MEASUREMENT OF SHEET RESISTANCE

The electrical resistance of SnO_2:F films was measured by two methods. Using indium-gallium eutectic and two copper wires to make two ohmic contacts to the film, the resistance between these two contacts of the film were measured using a multimeter. Follwing calibration, a two-point probe method (the separation of the probes was 1.0 cm) was used to measure the sheet resistance of the films.

3.6 ELECTROCHROMIC MEASUREMENT

The fabrication of the experimental ECC is shown in Fig.3.2. It consisted of a working electrode (WE), a counter electrode (CE) and an Ag/AgCl reference electrode (RE). The CE was a highly conductive SnO_2:F film (with sheet resistance of 20Ω/□) and the WE was polycrystalline WO_3 film on the SnO_2:F substrate. These two electrodes were fixed parallel to each other in a plexiglass frame leaving a 2 mm thick space, into which the electrolyte (10% H_2SO_4 in water

by volume) was placed. The RE was made by immersing a Ag wire in saturated KCl solution and applying a voltage of 1.0 to 1.5 V to the Ag wire with respect to a carbon counter electrode in the solution.

The electrochemical properties of the experimental ECC were studied using an instrumental arrangement of a lock-in amplifier (model HR-8); a potentiostat (model 173); an universal programmer (model 175); and an electrometer probe (model 178), all are produced by Princton Applied Research Co.. A x-y recorder (7000 AR, Hewlett Packard) and a monochromator (Industries Co., Metuchen, N.J.) were also used in the experiments. A PIN-6LC Scottky barrier silicon pin photodiode (United Detector Technology Inc., Santa Monica, Cal.) which has a linear response to visible and near-infrared lights was used to measure the light intensity transmitted through the cell. Fig.3.3 shows the block diagram of the apparatus used in the electrochemical measurements. The incident light source was a tungsten halogen lamp (Wild, Switzerland) which has a steady output intensity spectrum.

The voltage applied was between -0.5 and -1.5 V with respect to the Ag/AgCl reference electrode. The transmittance of each experimental cell was measured before and while the voltage was applied. The output spectrum of the monochromator without the cell was used as the reference spectrum. Also the transmittance of a reference cell made of two highly conductive SnO_2:F (without WO_3 layer) films was measured

before and while the voltage was applied.

White light was used to study the coloration time response of the cell during the voltage applied and to measure the transmittance as a function of the applied voltage.

As shown in Fig.3.3, the potentiostat in conjunction with the universal programmer was used (dotted line) in measuring the I-V characteristic of the cell.

Fig.3.1 The diagram showing the construction of the pyrolytic spray deposition oven

A: Spray Tube (aerosol source)

B: Aerosol Path

C: Electric Heater with Molten Tin Bath

F: Substrate

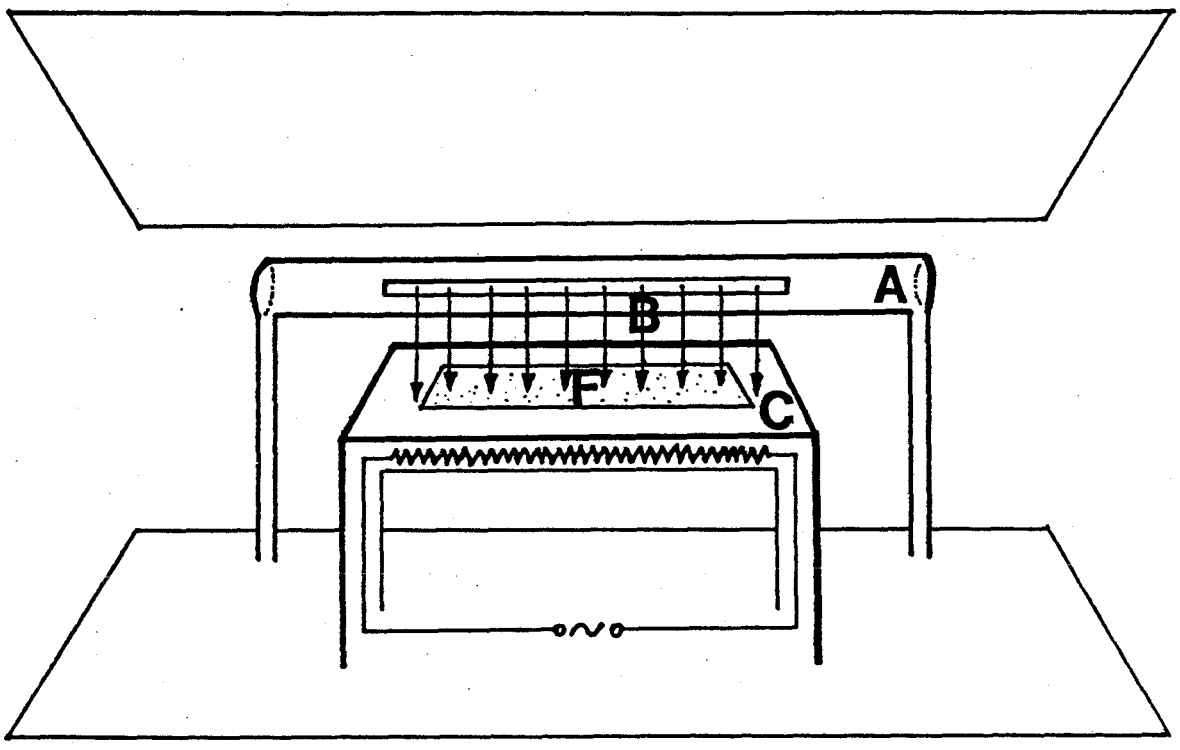

A: Spray Tube

B: Aerosol Path

C: Electric Heater

F: Deposited Film

Fig.3.2 The diagram of the cross-sectional geometry of the experimental cell

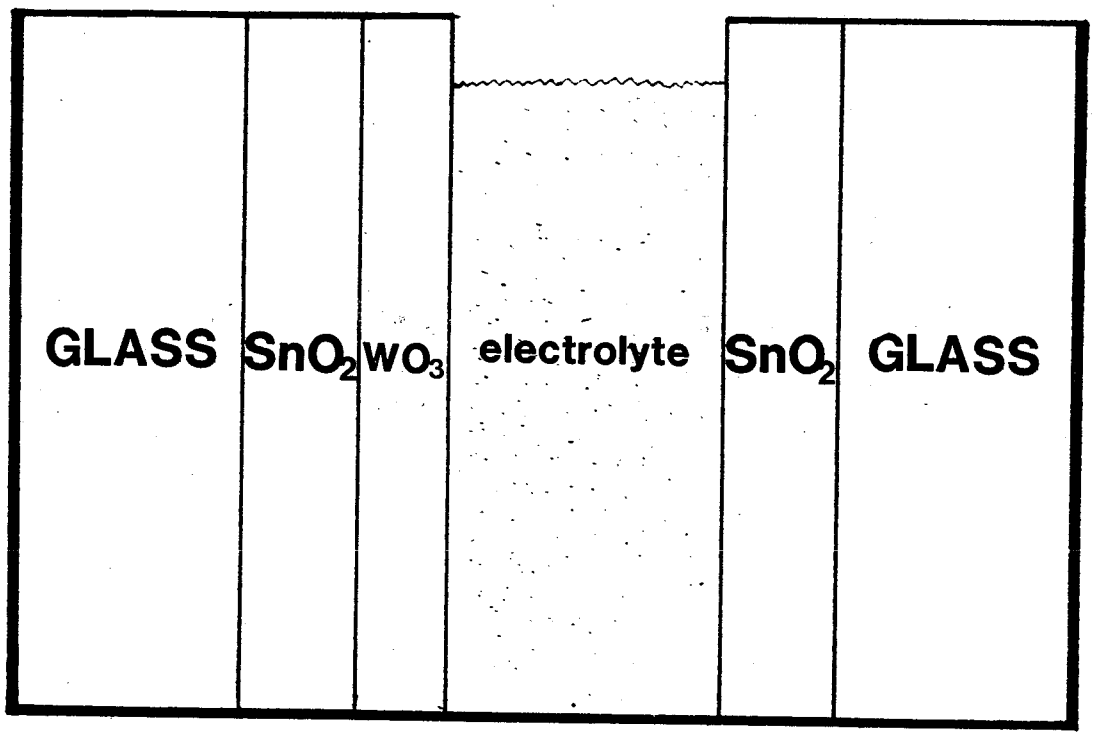
GLASS
SnO_2
WO_3
electrolyte
SnO_2
GLASS

Fig.3.3 The block diagram of electrochemical measurements

A: Tungsten Halogen Lamp

B: Filter

C: Chopper

D: Slit

E: Lens

ECC: Experimental Cell 1:working electrode,
2:reference electrode, 3:counter electrode

F: Detector

Dotted lines were connected when measuring the I-V characteristic of the cells.

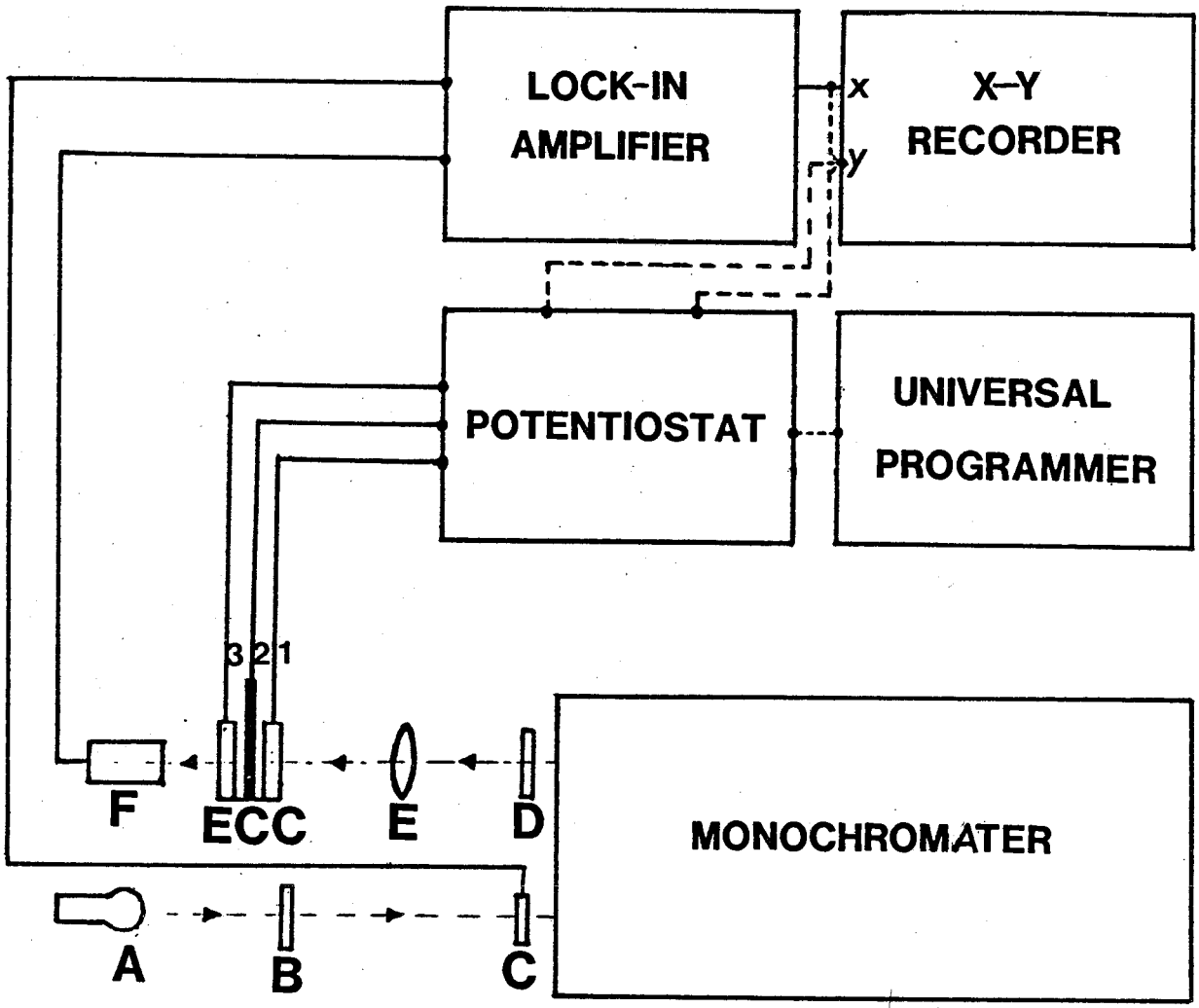

A: Tungsten Halogen Lamp

B: Filter

C: Chopper

D: Slit

E: Lens

ECC: Experimental Cell 1 working electrode, 2 reference electrode, 3 counter electrode

F: DETECTOR

CHAPTER 4

RESULTS AND DISCUSSION

4.1 PYROLYTICALLY SPRAY DEPOSITED SnO_2:F FILM

Fig.4.1 shows the X-ray diffraction patterns of four types of SnO_2:F films deposited at substrate temperatures T_s =300, 400, 450 and 500°C. It can be seen that the T_s dominates the film structure which shows amorphous,low polycrystalline, polycrystalline and highly polycrystalline structure respectively in the T_s range of 300°C to 500°C. SnO_2:F films are nonstoichiometric n-type semiconductors, their conductivity is due to the presence of a F donor level, Cl impurities, O vacancies and interstitial tin [45]. Table 4.1 lists the measured sheet resistance of several types of SnO_2:F films. Polycrystalline films (T_s = 450, 500°C) have a low sheet resistance of 20-50Ω/□ and amorphous film (T_s = 300°C) has a high sheet resistance of 10^7Ω/□. The reaction $SnCl_4 + 2H_2O \rightarrow SnO_2 + 4HCl$ is only complete at substrate temperature equal to or greater than 500°C, below 500°C the pyrolytic hydrolysis process of $SnCl_4$ presumably results in the formation of SnO_2, SnO, Cl_2, H_2 and O_2 [46]. It seems

that films deposited at T_s = 500°C are slightly less conductive than films deposited at T_s = 450°C. This may be due to a higher probability of Na^+ ions diffusing from the glass substrate into the SnO_2:F film and thereby creating acceptor centers and forming larger NaCl crystals in the films deposited at a higher substrate temperature during the deposition. The acceptor centers in the film can decrease the net carrier concentration and therefore decreasing the conductivity [45]. Further, the degree of crystallinity of SnO_2:F films increases with the increase of T_s up to 500°C, the X-ray diffraction peaks showed the same preferred orientation along the normal direction of the (200) plane perpendicular to the surface of the film for all polycrystalline SnO_2:F films. This observation is consistent with the results of Fantini et al. [47].

As shown in the Table 4.1, the thicknesses of all types of SnO_2:F films deposited are greater than 5000Å, which are thick enough to eliminate the size effect on conductivity of the film at thickness about 4000Å [45].

Fig. 4.2 presents the transmittance spectra of a SnO_2:F film deposited at T_s = 500°C with a thickness of 5380Å . The average visible transmittance is greater than 80% which is highly desirable as the substrate for electrochromic coatings. The F doping concentration may be used to control both conductivity and transmittance of SnO_2:F films. Islam et al. [45] found that an increasing doping impurity

concentration results in an increased conductivity and decreased transmittance of SnO_2:F films. So by choosing a proper doping level and appropriate substrate temperature, high quality transparent conducting SnO_2:F films can be obtained and used as substrate films for electrochromic layers and as a counter electrode in ECCs.

4.2 PYROLYTICALLY SPRAY DEPOSITED WO_3 FILM

As shown in Fig.4.3, the angle positions of X-ray diffraction peaks of H_2WO_4 powder before and after being heated at a temperature of 450°C for 10 hours are completely different. According to eq. (3.7), this might imply that H_2WO_4 powder becomes WO_3 powder and water vapor during heating. By comparing the diffraction patterns of the heated H_2WO_4 powder and the WO_3 film deposited onto a glass from a tungsten chloride solution at a substrate temperature of 450°C (Fig.4.3), it was found that the main peaks corresponding to the WO_3 crystal planes [001], [020] and [111] at the positions 2θ = 23.2, 23.8 and 28.3° respectively compare well in these two samples. In addition, some peaks at positions 2θ = 21.7, 38.8 and 56.2° in the diffraction pattern of the WO_3 film deposited onto a glass slide from a tungsten chloride solution may be assigned to the sub-oxides WO_{3-x} ($o<x<3$) [10], [11]. However, the pyrolytically spray deposited

tungsten oxide films have a main composition of tungsten trioxide. This was also confirmed by XPS measurement by Craigen et al. [14].

X-ray diffraction also revealed that WO_3 films deposited onto glass slides at T_s = 350 and 400°C are amorphous and at T_s = 450°C are polycrystalline in nature; WO_3 films deposited onto SnO_2:F at T_s from 360 to 470°C are polycrystalline in nature. This is consistent with the prior report of pyrolytically spray deposited WO_3 films [14]. It was also found that the main peaks of the diffraction patterns of all pyrolytically spray deposited WO_3 films correspond to the WO_3 crystal planes [001], [020], [200] and [111] at the angle positions 2θ = 23.2, 23.8, 24.4 and 28.3° respectively. However, other peaks such as WO_3 [021], [221], [002], etc. and some peaks of other types of tungsten oxides were also observed in the diffraction patterns of some films. These observations show excellent agreement with those of evaporated and sputtered WO_3 films [9], [10].

4.2.1 Thickness and Resistivity of WO_3 Films

Table 4.2 lists the measured values of thicknesses of WO_3 films deposited using different deposition parameters. Thicknesses of films ranging from 380 to 4140±20% Å are related to the deposition time and carrier gas N_2

flowrate. But it is not a linear relationship with respect to these two parameters. It seems that the substrate temperature during deposition influences the crystallinity of the films, and also affects the thickness of the film. This may be due to the fact that a different degree of crystallinity of the WO_3 films may result in a different density of the films [11]. The uncertainty in the thickness measurements is about 20%. The thickness measurements by the mechanical " taly-step " technique compared well with those by the interference step technique within the uncertainty of about 20%.

The resistivity of WO_3 films was obtained by measuring the sheet resistance of films of tungsten chloride solution deposited onto glass slides. The following three WO_3 films were obtained by depositing the tungsten chloride solution the onto glass slides with a N_2 flowrate of 16.5 l./min for 10 minutes at various substrate temperatures:

sample	T_s(°C)	thickness(Å)	sheet resistance(Ω/□)
WG1	300	2200	$>10^9$
WG2	350	2300	10^8
WG3	450	2900	10^4

X-ray diffraction patterns revealed that WG1 and WG2 are amorphous and WG3 is polycrystalline in nature. From the sheet resistance and thickness as well as the dimensions of

above three films it is estimated that the amorphous film has a resistivity of about $2.3X10^4$ Ωcm and the polycrystalline film has a resistivity of about 0.3 Ωcm. These values are a little lower than those of vacuum evaporated films reported by Miyake et al. [10]. Possibly this was due to the incomplete decomposition of WCl_6 in our case.

The sheet resistance of the WO_3 films deposited onto SnO_2:F were not determined since the SnO_2:F film has a much lower resistivity than the WO_3 films and thus acts as a short.

4.2.2 Crystallinity of WO_3 Film

The carrier gas N_2 flowrate has a prominent effect on the crystallinity of WO_3 films. Fig.4.4 illustrates the difference in the X-ray diffraction patterns of three WO_3 films deposited onto highly polycrystalline (T_s = 500°C) SnO_2:F at a substrate temperature of 400°C for 7 minutes with N_2 flowrates of 7.5, 16.5 and 38 l./min respectively. Although all these three films were polycrystalline in nature, the film deposited with a N_2 flowrate of 16.5 l./min has a more randomly oriented crystallite structure since more diffraction peaks appeared. Further, as shown in the following table, the film deposited with a N_2 flowrate of 16.5 l./min has the largest crystallite size (corresponding to the [001] plane) in structure.

N_2 flow.(l./min)	nebul. rate(ml./min)	cryst.size(Å)	thick.(Å)
7.5	2.5	215	380
16.5	6.5	760	2230
38.0	10.5	639	3480

The nebulization rate was determined by measuring the initial and final volume of the tungsten chloride solution.

The speed of the aerosol droplets which is proportional to the carrier gas flowrate affects the deposition rate and hence the structure of the deposited films [48]. There may be an optimum value of nebulization rate for the crystallite size and orientation randomness of films within the range of the nebulization rate used . The dependence of crystallite size on the nebulization rate (related to deposition rate) shows a maximum value which is consistent with the prediction of Chopra for vapor-deposited polycrystalline films [48].

Fig.4.5 shows the difference of the X-ray diffraction patterns between WO_3 films deposited onto four types of SnO_2:F substrates (shown in Fig.4.1) at T_s = 400°C with N_2 flowrate 16.5 l./min for 7 minutes. It was found that the higher crystallinity of the SnO_2:F substrate results in a higher crystallinity of the WO_3 film itself; films deposited onto the SnO_2:F at T_s = 450°C show a more randomly oriented crystallite structure than those deposited at other

temperatures as can be seen in Fig. 4.5. The dependence of the crystallite size corresponding to the main peaks on the nature of substrate is shown as following:

T_s of SnO_2(°C)	cryst.size(Å)±20% [001]	[020]	[200]
300	392	220	/
400	355	220	202
450	760	760	760
500	760	392	760

The nature and smoothness of the substrate surface can influence the atomic mobility and diffusion of surface atoms during the deposition and hence the crystalline structure of film deposited [47].

The substrate temperature is an important deposition parameter which influences the crystallinity of polycrystalline films. The average crystallite size corresponding to [001] plane vs substrate temperature of films deposited onto amorphous (T_s = 300°C) and highly polycrystalline (T_s = 500°C) SnO_2:F substrate is presented in Fig.4.6. Using the measurement uncertainty of $\Delta(2\theta) = 0.05°$ in measuring the half maximum broadening of the diffraction peaks, the average crystallite sizes calculated by eq. (3.5) and (3.6) were on the order of 200 to 760 Å. However, the crystallite size of some well crystallized films

may be larger than 760 Å in the limiting case when B_M approaches B_S. As shown in Fig. 4.6, the crystallite size of films deposited onto a amorphous substrate slightly decreases with the increase of T_s from 400 to 470°C, and for highly polycrystalline substrates increases with the increase of T_s from 360 to 420°C and then decreases with the increase of T_s from 420 to 470°. This dependence of crystallite size on the substrate temperature of WO_3 films is somewhat different from the observation reported for some films deposited by other methods, such as SnO_2 film [49]. Chopra [48] predicated theoretically that the crystallite size of most polycrystalline films would increase with substrate temperature during deposition or annealing. Maudes et al. [49] reported that the crystallite size of polycrystalline SnO_2 film increased with increasing substrate temperature. In contrast to Chopra, Achrya et al.[50] showed that the crystallite size of MnO_2 films decreases with annealing temperatures from 113 to 305°C and then increases with annealing temperatures from 305 to 413°C. The crystallite size of pyrolytically spray deposited WO_3 films has a maximum value at the substrate temperature of about 420°C as seen in Fig.4.6. For large scale production of electrochromic coatings a lower substrate temperature is desirable to maintain low costs. Moreover, at high substrate temperatures, the Na^+ ions may diffuse from the glass substrate into the SnO_2:F film, thereby reducing the conductivity of SnO_2:F film. However, a high substrate conductivity is very

important for electrochromic windows.

Chopra [48] also expected that the crystallite size of polycrystalline films increases with thicknesses up to a certain value and then keeps constant with increasing film thickness [48]. As shown in Fig.4.7, the [001] plane crystallite size of WO_3 films deposited onto highly polycrystalline (T_s = 500°C) SnO_2:F substrate shows no trend with increasing film thickness up to about 1000Å but increases to a plateau at greater film thicknesses. Amorphous (T_s = 300°C) SnO_2:F substrate also shows the same crystallite size distribution of WO_3 films with different film thicknesses although there are not sufficient experimental data available. This observation agrees with Chopra [48] in spite of the fact that substrate temperature and the nebulization rate were not kept constant during the deposition. The crystallite sizes corresponding to the main diffraction peaks of WO_3 films deposited onto polycrystalline (T_s = 450°C) SnO_2:F substrate at T_s = 420°C with N_2 flowrate 16.5 l./min seem to be independent of film thickness from 1200 to 4300Å except for a few scattered points of the [001] and [020] planes (Fig.4.8). This may be because the thicknesses of this group of films are greater than crystallite size.

So far it is concluded that WO_3 film deposited onto polycrystalline (T_s = 450°C) SnO_2:F film at substrate temperature 420°C with N_2 flowrate of 16.5 l./min shows the larger crystallite size and more randomly oriented crystallite

structure. The following discussion will therefore concentrate on films deposited under these conditions but with different deposition times, i.e. different thicknesses of the WO_3 films.

Preferential orientation of crystallites is an important phenomenon in polycrystalline thin films, especially the thickness effects on the orientation [48]. A preferentially oriented crystal face corresponds to the lowest surface free energy of the crystal. WO_3 films, which have a hexagonal close-packed (octahedron) crystal structure , are expected to show a [001] preferential orientation [51]. As shown in Fig.4.9 the diffraction peak intensities of the [001] and [020] planes are stronger than those of the [200] and [111] planes for WO_3 films deposited onto polycrystalline SnO_2:F at T_s = 450°C with a N_2 flowrate of 16.5 l./min . However, the intensities of the [001], [200] and [111] planes had the same distribution with a maximum value at thicknesses of about 2500Å and the intensity of the [020] plane increased rapidly with thicknesses greater than 2500Å. By taking the ratio of diffraction peak intensities of the [001] and [020] planes to other planes respectively (Fig.4.10 and Fig.4.11), it was found that the [001] plane showed a preferred orientation for film thicknesses of 1200 to 2500Å while the [020] plane was highly preferential oriented for film thicknesses 3000 to 4300Å. Further, films of thicknesses of approximately 2900Å showed a more randomly oriented crystallite structure although they still showed a slight

the [020] preferred orientation.

4.3 ELECTROCHROMIC BEHAVIOR OF WO_3 FILM

4.3.1 Visible and Near Infrared Transmittance

As shown in Fig.4.2, the visible average transmittance of a polycrystalline WO_3 film deposited onto highly polycrystalline (T_s = 500°C) SnO_2:F film at substrate temperature of 440°C with a thickness 440Å is about 70%. The remaining 30% may be due to reflection [18] or absorption [16], or both. After applying a voltage (measured between WE and RE) to the ECC, it was observed that WO_3 films deposited onto highly conducting (T_s = 450, 500°C) SnO_2:F substrates showed a blue coloration . The degree of color depends on the voltage applied and with the increasing negative bias of the working electrode the transmittance reduced remarkably; WO_3 films deposited onto amorphous (T_s = 300°C) substrate showed no visible coloration and the transmittance changed little. This maybe due to the high resistivity of the substrate (see Table 4.1).

Fig.4.12 illustrates the thickness dependence on the transmittance change at three wavelengths (5500, 6330 and 9000Å) for films deposited onto highly conducting (T_s = 450°C) SnO_2:F at a substrate temperature of 420°C with N_2

flowrate of 16.5 l./min. The voltage applied was -0.5V. It was found that the crystallite orientation of the films has a strong influence on the transmittance change during the coloration . The visible (5500Å) transmittance change increased from about 10% to 65% and then decreased to 20%; and the near infrared (9000Å) transmittance change increased from about 50% to 90% and then decreased to 50%. The transmittance change was obtained by comparing the transmission spectra of before and during coloration for each experimental cell. Because the transmission spectra of every cells do not show interfernce effects, in Fig.4.12 the peaks at film thickness about 3000Å can not be due to interfernce effect. The variation in transmittance change corresponds to the crystallite orientation changing from [001] preferred orientation to a randomly oriented crystallite state (slight [020] preferred orientation) and then to the highly [020] preferred orientation state. It seems that the [001] crystallite preferred orientation has a stronger influence on the electrochromic behavior than the [020] crystallite preferred orientation of the WO_3 film. Joo et al. [52] measured the lithium diffusion coefficients in electrochemically grown $K_{0.28}WO_3$ single crystal along the $\vec{a}$ and $\vec{c}$ crystallographic direction. They reported that the lithium diffusion coefficient for the $\vec{c}$ crystallographic direction is $10^{-8}cm^2/sec$, which is one order of magnitude lower than that along the $\vec{a}$ crystallographic direction. The

lithium diffusion coefficient in $K_{0.28}WO_3$ single crystal along the b crystallographic direction has not been reported yet. However it may be higher than that along the c crystallographic direction because in a hexagonal close-packed (octahedron) structure the crystal face of the c crystallographic direction [001] corresponds to the lowest surface free energy, thereby the smallest atomic diffusion coefficient along this direction. The difference of influence on the transmittance change between the WO_3 films with [001] and [020] preferred crystallite orientation is consistent with the results reported by Joo et al. [52]. Referring to Fig.4.9, the unusual low points at thickness 2550Å in Fig.4.12 may be reasonable because this film showed an unusual high [001] preferred crystallite orientation structure. The infrared transmittance changed more than the visible transmittance because injected electrons in polycrystalline WO_3 film show near free electron behavior [4], [7], [15]. The transmittance change dependence on crystallite orientation of the films can be understood phenomenologically: polycrystalline films consist of crystallite domains, preferentially oriented crystallites have a smaller angle between grain boundaries. Then with the same voltage applied , films of randomly oriented crystallite with larger angle between grain boundaries could have more cations and electrons injecting into film through grain boundaries than films with preferentially oriented crystallites and thus results in higher reflection and thus a larger transmittance

change.

Fig.4.13 shows the dependence of the transmittance change on crystallite size for four films with thicknesses of 2550, 2600, 2780 and 3100Å. The transmittance change increased rapidly with increasing crystallite size. The electrons injected into films with larger crystallite size show more likely free-electron behavior (less grain boundary scattering) which results in higher reflection and thus a larger transmittance change. Although there were only four experimental data points available in Fig.4.13, the tendency of the relation between transmittance change and crystallite size supported the hypothesis of Svensson et al [6], [7]. On the basis of spectroscopic ellipsometry studies and an analysis of the dynamical resistivity of colored polycrystalline WO_3 film and single crystal Na_xWO_3, Goldner et al. [53] estimated that the reflection of the single crystal Na_xWO_3 is twice as that of the polycrystalline WO_3 film in the visible and near infrared region. This may also imply that the higher crystallinity of polycrystalline WO_3 films results in higher reflection during coloration.

As expected, the transmittance of the reference cell (without WO_3 layer) did not change with applied voltage. Schirmer et al. [16] reported that the optical density of polycrystalline WO_3 film increases 50% only during electrochemical coloration, thus it was believed that the transmittance change of pyrolytically spray deposited

polycrystalline WO_3 film during the coloration was mainly due to an increase in reflection, which was confirmed by us in some preliminary measurements using a He-Ne laser.

4.3.2 I-V Characteristics of ECC

A typical cyclic voltammogram of a WO_3 electrochromic cell is presented in Fig.4.14. The WO_3 film of this cell was deposited onto highly conducting (T_s = 450°C) SnO_2:F at a substrate temperature of 420°C with a N_2 flowrate of 16.5 l./min. This film has a thickness of 2780A with randomly oriented crystallites structure (760Å crystallite size corresponding to main crystal planes). The effective area of this cell was 0.2cm X 0.25cm. As shown in Fig.4.14, the voltage sweep starts from the spontaneous potential of -0.12V vs Ag/AgCl, which was found to be the rest potential under open-circuit condition. At the threshold potential of about -0.3V, the cathodic current causes a coloration reaction of the WO_3 film, which was also reported by other authors [54]. At the turning point (-10.5V), the cathodic current attains a peak value of 4mA/cm². At the potential of -0.75V the anodic current which is associated with the bleaching reaction begins to appear, it increases to a peak value of 2.3A/cm² at the potential of about -0.65V and then decreases dramatically untill bleaching is nearly complete at the potential of about -0.5V.

After one voltammogram cycle is completed, the cell returns to its initial state with a small residual anodic current of about 0.2mA/cm². The second cycle is almost the same as the first one.

The I-V characteristics of the cell are consistent with the white light transmittance of the cell as a function of the voltage applied as shown in Fig.4.15. The transmittance begins to drop at a potential of about -0.3V, which corresponds to the onset of coloration in Fig.4.14. The transmittance did not return to its initial value because the rather high scan rate (20mV/Sec.) results in incomplete bleaching.

Fig.4.16 presents the time response of the same experimental cell discussed above. The white light transmittance decreased 56% within 25 seconds after a bias of -0.5V applied and then reached a nearly steady transmission value of 20% in about 2 minutes. Due to the high ion mobility of the liquid electrolyte used, the bleaching time corresponding to 56% of the transmission was about 60 seconds under short circuit condition and 50 seconds with +0.5V applied. After +0.5 voltage applied for 5 minutes the cell returned to its initial clear state. Although the time response is much slower than that of amorphous WO_3 electrochromic display devices [55], it is acceptable for the purpose of " smart windows ".

Table 4.1 SnO_2:F films deposited onto glass slides with a N_2 flowrate of 38.0 l./min

T_s (°C)	time (min)	thick.(Å)	sheet R ($\Omega/\square$)
300	20	6050±20%	$7X10^6$
350	20	7850±20%	$5X10^3$
400	20	8500±20%	$1X10^2$
450	15	7700±20%	20
500	10	5380±20%	50

Table 4.2-1 WO3 films deposited onto amorphous SnO2:F (T_s =300°C, R = 7X10^{6}Ω/□, thickness = 6050Å)

T_s(°)	N_2 flow.(l./min)	time(min)	thick.(Å)±20%
400	7.5	7	580
400	16.5	7	1560
400	38.0	7	2310
420	7.5	10	610
440	7.5	10	730
460	7.5	10	800
470	7.5	10	850

Table 4.2-2 WO_3 films deposited onto low polycrystalline SnO_2:F (T_s = 400°, R = 100Ω/□, thickness = 8500Å)

T_s(°C)	N_2 flow.(l./min)	time(min)	thick.(Å)±20%
400	7.5	7	610
400	16.5	7	1560
400	38.0	7	2890
360	7.5	10	630
380	7.5	10	870
400	7.5	10	1100
420	7.5	10	1150
440	7.5	10	1270
460	7.5	10	1380
470	7.5	10	1450

Table 4.2-3 WO_3 films deposited onto highly polycrystalline SnO_2:F (T_s = 500°, R = 50Ω/□, thickness = 5380Å)

T_s(°C)	N_2 flow.(l./min)	time(min)	thick.(Å)±20%
400	7.5	7	380
400	16.5	7	2230
400	38.0	7	3480
360	7.5	10	410
380	7.5	10	
400	7.5	10	400
420	7.5	10	370
440	7.5	10	440
460	7.5	10	360
470	7.5	10	520

Table 4.2-4 WO_3 films deposited onto polycrystalline SnO_2:F (T_s = 450°C, R = 20Ω/□, thickness = 7700Å) at a substrate temperature of 420°C with a N_2 flowrate of 16.5 l./min

time (min.)	thickness (Å) ± 20%
1	1160
2	1473
3	1680
6	2310
8	2550
10	2600
10	2780
13	3100
15	3312
20	4140

Fig.4.1 X-ray diffraction patterns of four types of SnO_2:F films deposited onto glass slides with a N_2 flowrate of 38.0 l./min

type	substrate temperature (°C)
A	300
B	400
C	450
D	500

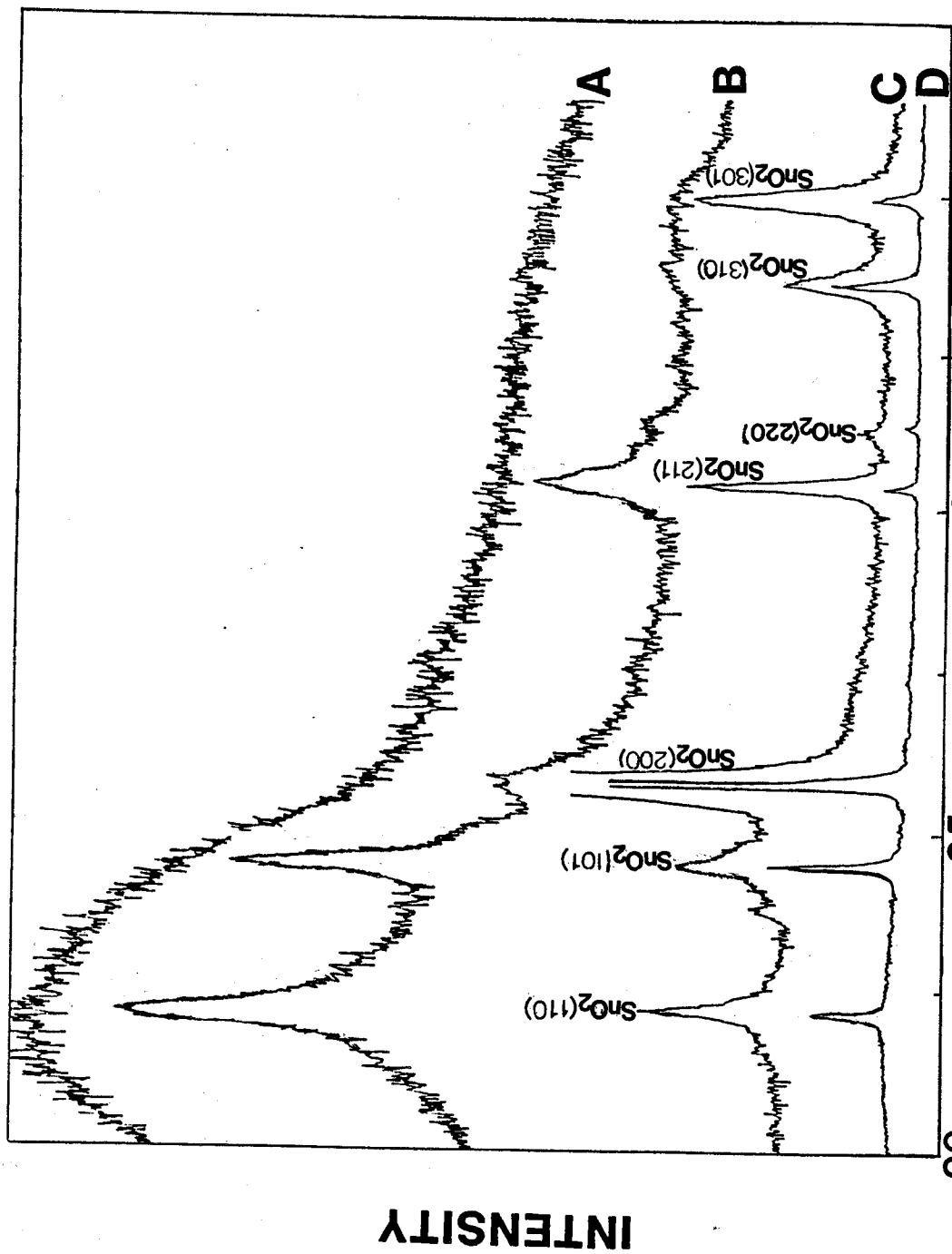
A
B
C
D
SnO2(110)
SnO2(101)
SnO2(200)
SnO2(211)
SnO2(220)
SnO2(310)
SnO2(301)
20
35
50
65
INTENSITY
DIFFRACTION ANGLE (2θ)

Fig.4.2 Normal transmittance spectra of a highly polycrystalline SnO_2:F film deposited onto glass with thickness 5380Å and a WO_3 film deposited onto the above SnO_2:F film with a thickness of 440Å

A: SnO_2:F film

B: WO_3 film on SnO_2:F

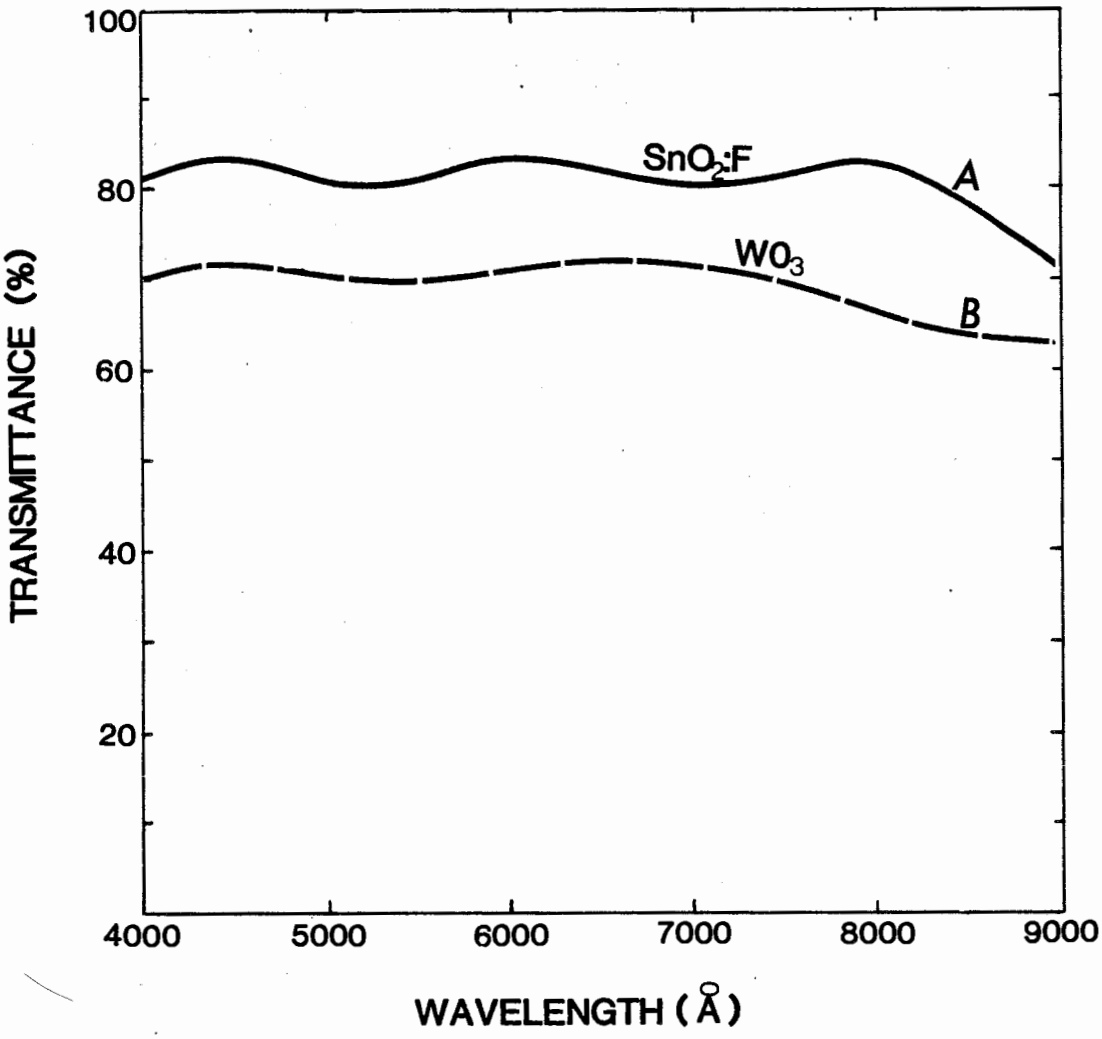
100
80
60
40
20
TRANSMITTANCE (%)
SnO2:F
A
WO3
B
4000
5000
6000
7000
8000
9000
WAVELENGTH (Å)

Fig.4.3 X-ray diffraction patterns

A: WO_3 deposited onto a glass slide at T_s = 450°C with a N_2 flowrate of 16.5 l./min for 7 minutes

B: H_2WO_4 powder heated at temperature 450°C for 10 hours

C: H_2WO_4 powder untreated

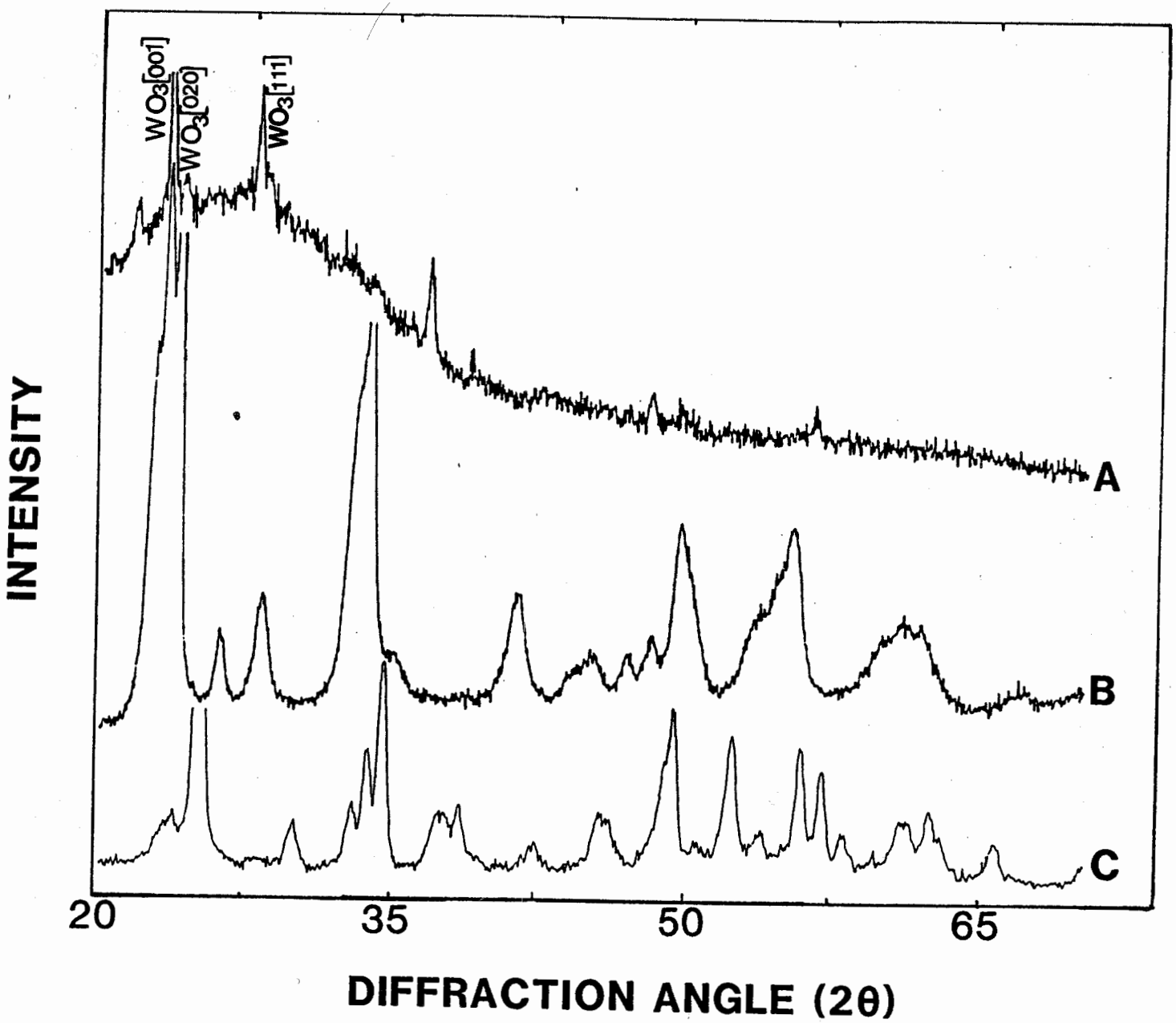
WO3[001]
WO3[020]
WO3[111]
INTENSITY
A
B
C
20
35
50
65
DIFFRACTION ANGLE (2θ)

Fig.4.4 X-ray diffraction patterns of WO_3 films deposited onto highly polycrystalline (T_s = 500°C) SnO_2:F at a substrate temperature of 400°C for 7 minutes

A: N_2 flowrate 16.5 l./min

B: N_2 flowrate 7.5 l./min

C: N_2 flowrate 38.0 l./min

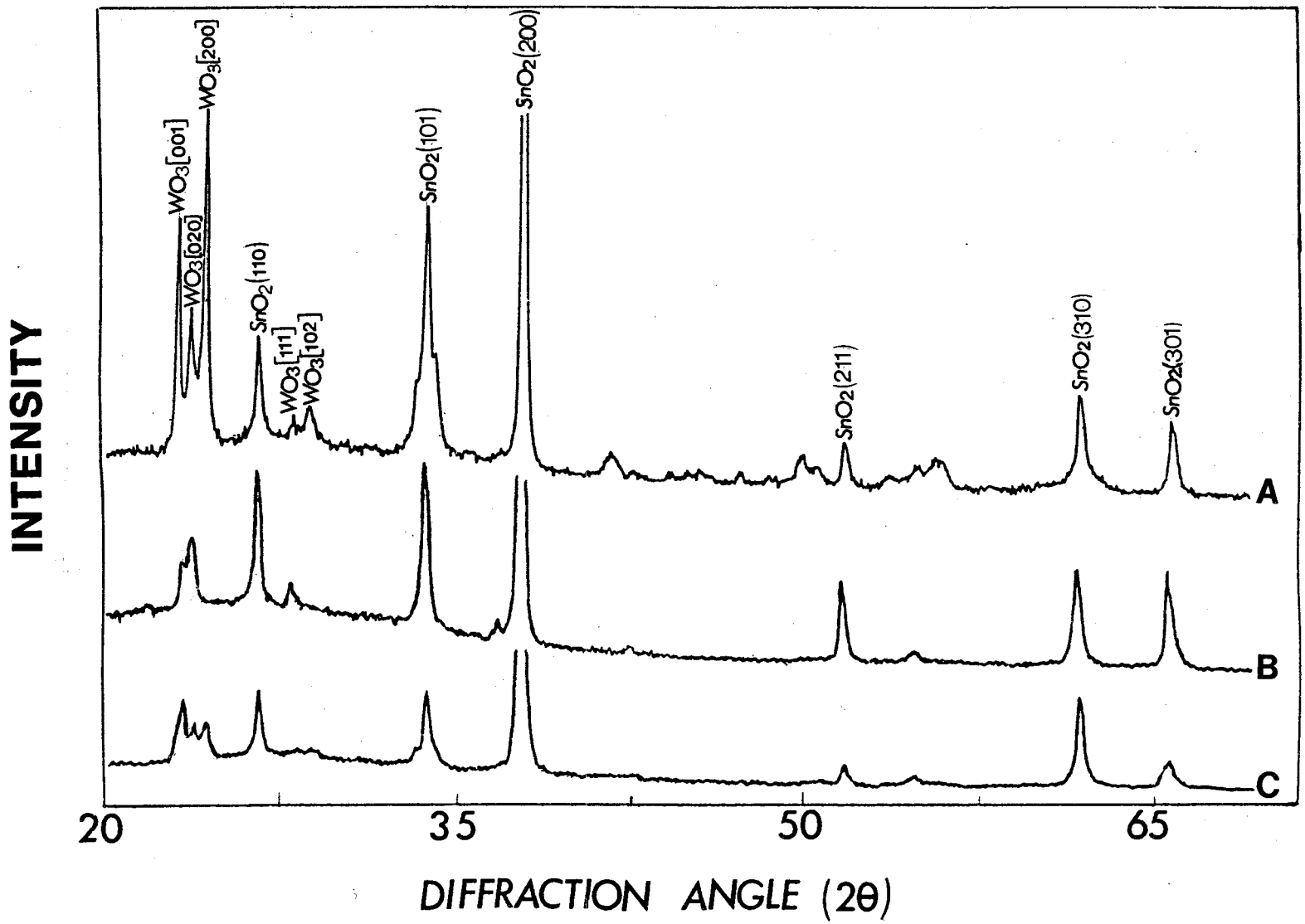
INTENSITY
WO3[001]
WO3[020]
WO3[200]
SnO2(110)
WO3[111]
WO3[102]
SnO2(101)
SnO2(200)
SnO2(211)
SnO2(310)
SnO2(301)
A
B
C
20
35
50
65
DIFFRACTION ANGLE (2θ)

Fig.4.5 X-ray diffraction patterns of WO_3 films deposited onto four types of SnO_2:F substrates (as shown in Fig.4.1) at T_s 400°C with N_2 flowrate 16.5 l./min

sample	T_s of SnO_2:F (°C)
A	300
B	400
C	450
D	500

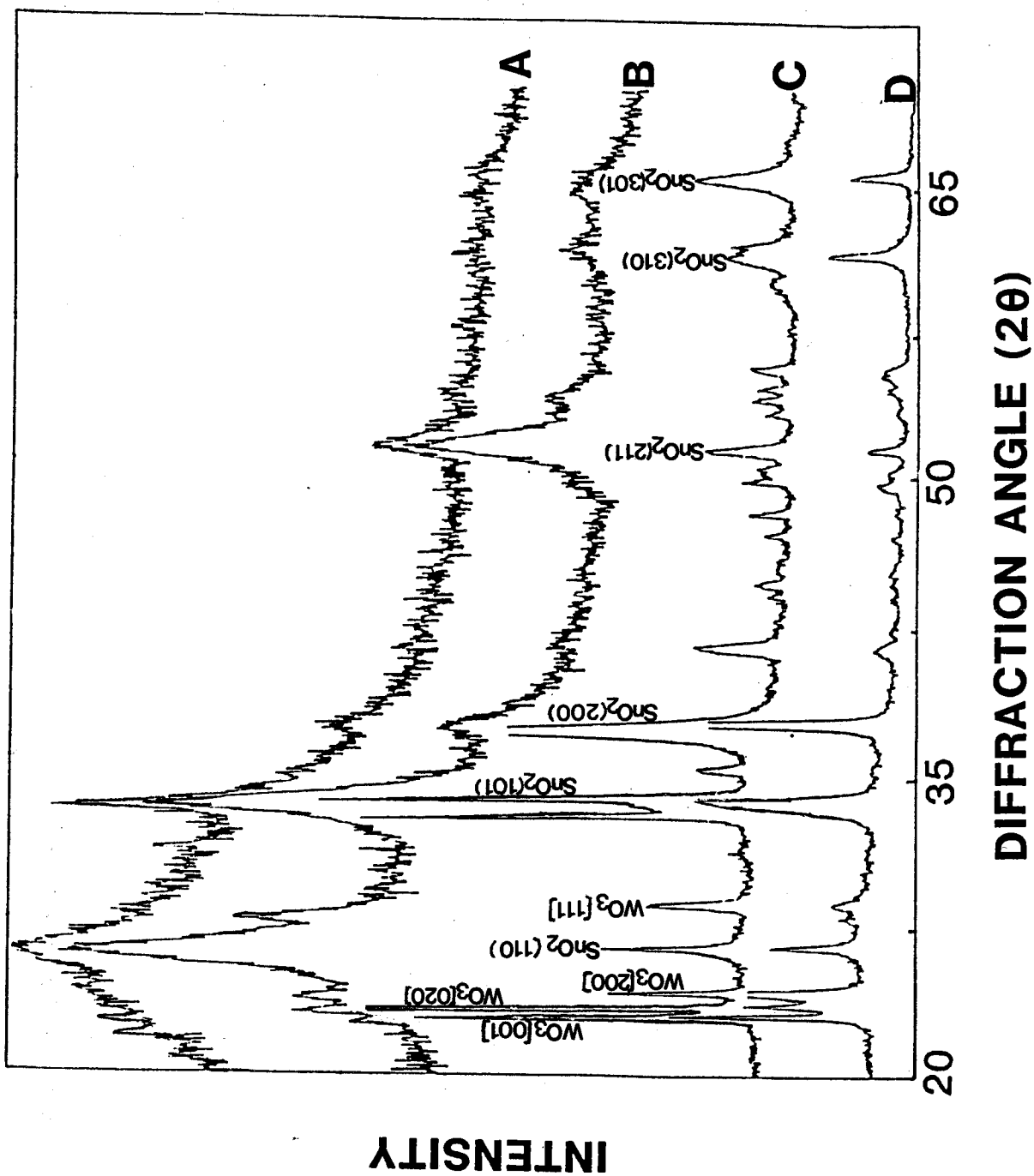
A
B
C
D
WO3[001]
WO3[020]
WO3[200]
SnO2 (110)
WO3[111]
SnO2(101)
SnO2(200)
SnO2(211)
SnO2(310)
SnO2(301)
20
35
50
65
DIFFRACTION ANGLE (2θ)
INTENSITY

Fig.4.6 Dependence of crystallite size (corresponding to the [001] plane) on the substrate temperature of WO_3 films

○ A: deposited onto amorphous (T_s =300°C) SnO_2:F

● B: deposited onto highly polycrystalline (T_s = 500°C) SnO_2:F

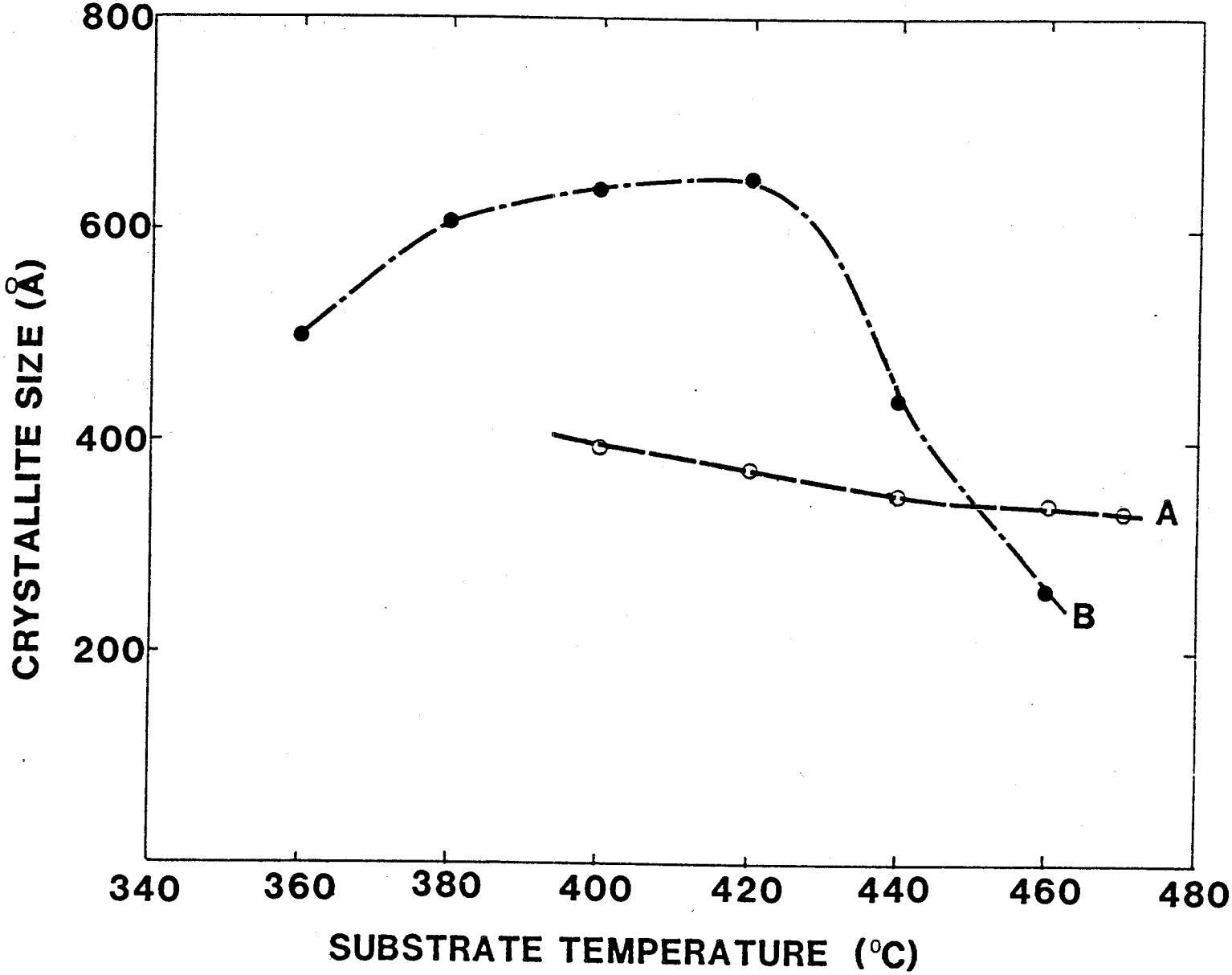
800
600
400
200
CRYSTALLITE SIZE (Å)
340
360
380
400
420
440
460
480
SUBSTRATE TEMPERATURE (°C)
A
B

Fig.4.7 Dependence of the crystallite size (corresponding to the [001] plane) on the thickness of WO_3 films deposited at substrate temperatures ranging from 360 to 470°C

● A: highly polycrystalline (T_s = 500°C) SnO_2:F substrate

○ B: amorphous (T_s = 300°C) SnO_2:F substrate

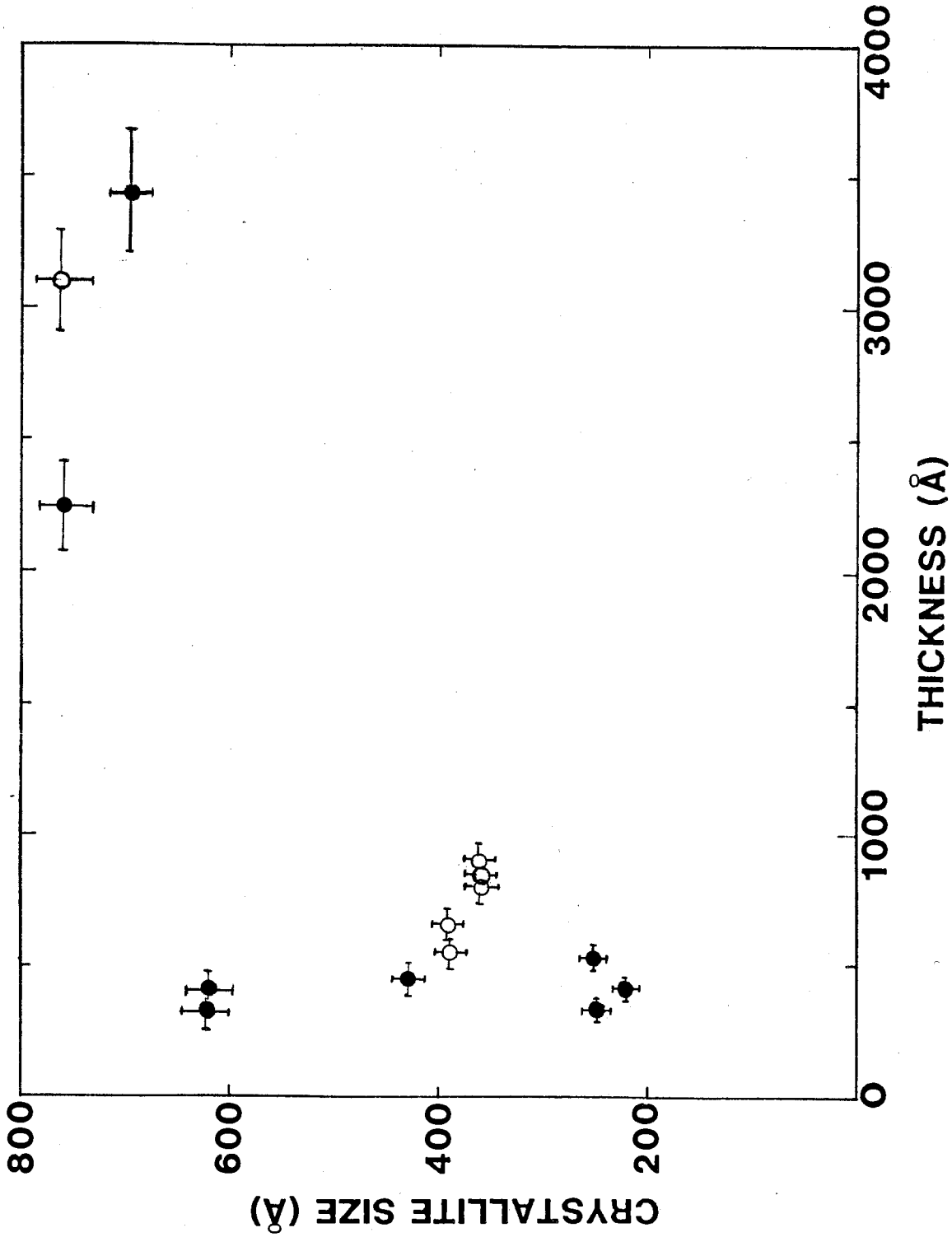
CRYSTALLITE SIZE (Å)
800
600
400
200
0
1000
2000
3000
4000
THICKNESS (Å)

Fig.4.8 Dependence of the crystallite size on the thickness of WO_3 films deposited onto polycrystalline (T_s = 450°C) SnO_2:F at a substrate temperature of 420°C with N_2 flowrate 16.5 l./min

● [001]

○ [200]

▲ [111]

For [020] plane the crystallite sizes of all films are about 760Å. The error bars for some points close to each other are not shown, and are similar to the error bars indicated.

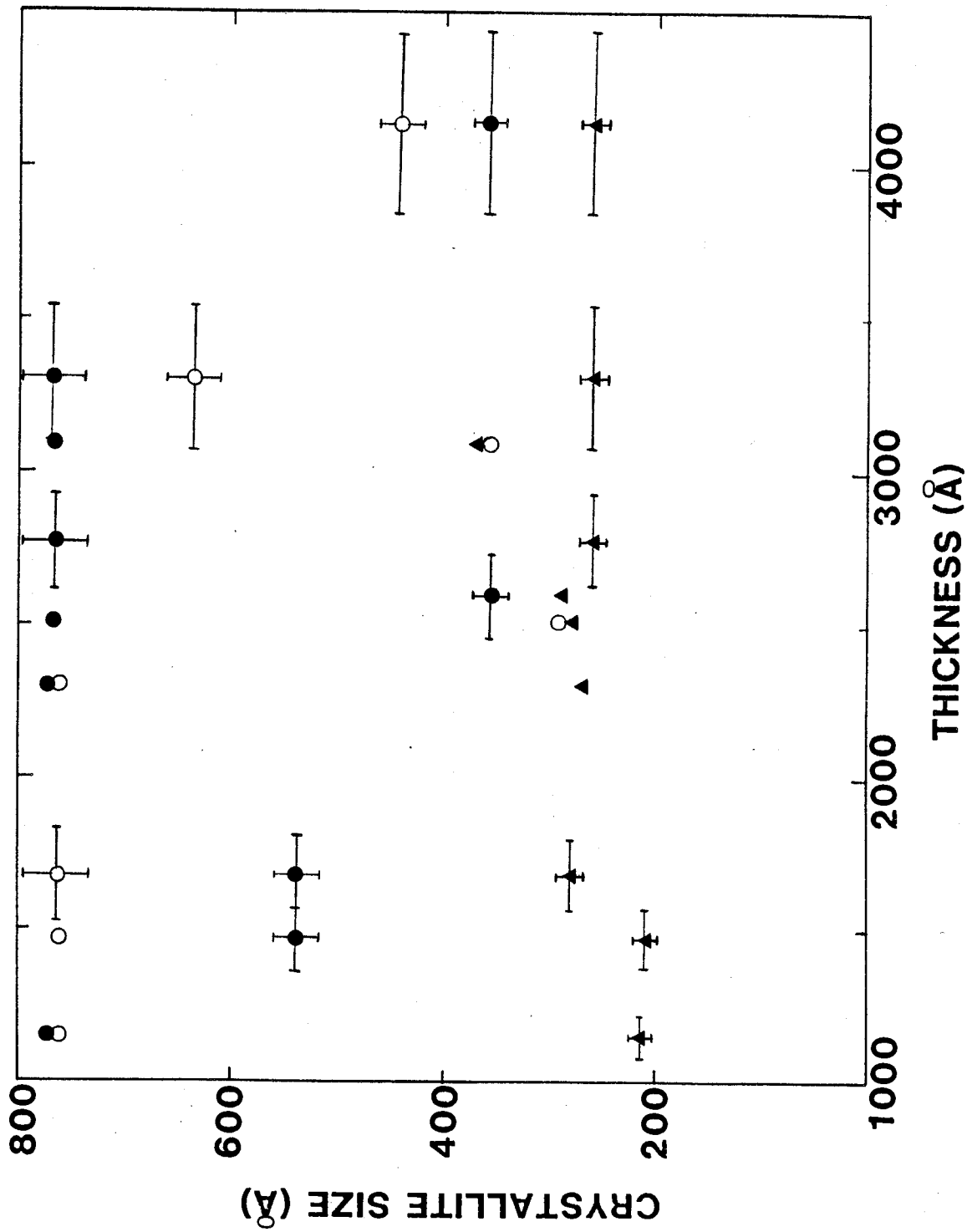
CRYSTALLITE SIZE (Å)
800
600
400
200
1000
2000
3000
4000
THICKNESS (Å)

Fig.4.9 Diffraction peak intensity distribution with thickness of the same WO_3 films as in Fig.4.8

● A: [001]

○ B: [002]

▲ C: [111]

△ D: [020] The actual intensity is 8 larger than shown.

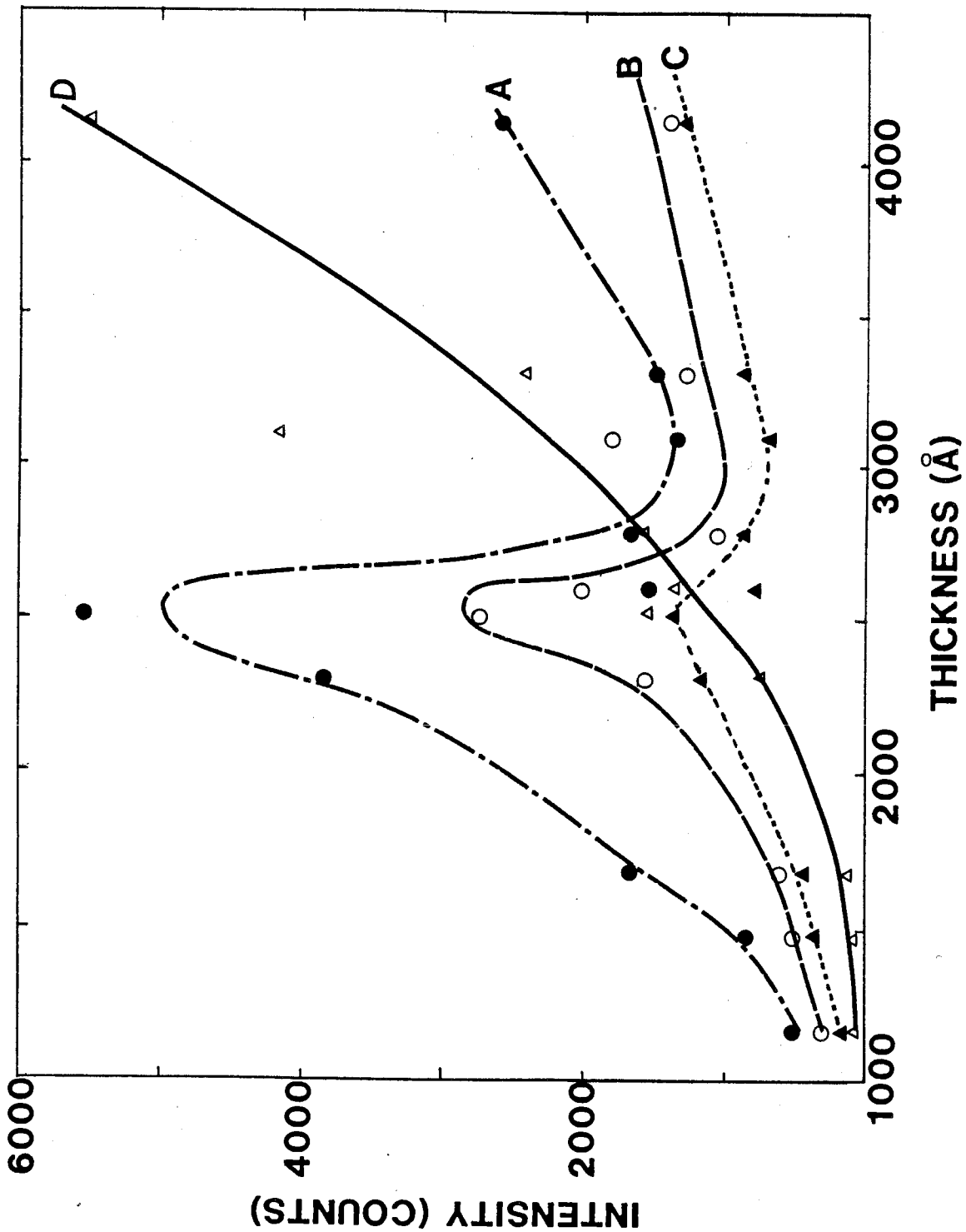
INTENSITY (COUNTS)
6000
4000
2000
1000
2000
3000
4000
THICKNESS (Å)
A
B
C
D

Fig.4.10 Dependence of the intensity ratio on the thickness of the same WO_3 films as in Fig.4.9

● A: [001]/[111]

○ B: [001]/[002]

▲ C: [001]/[020]

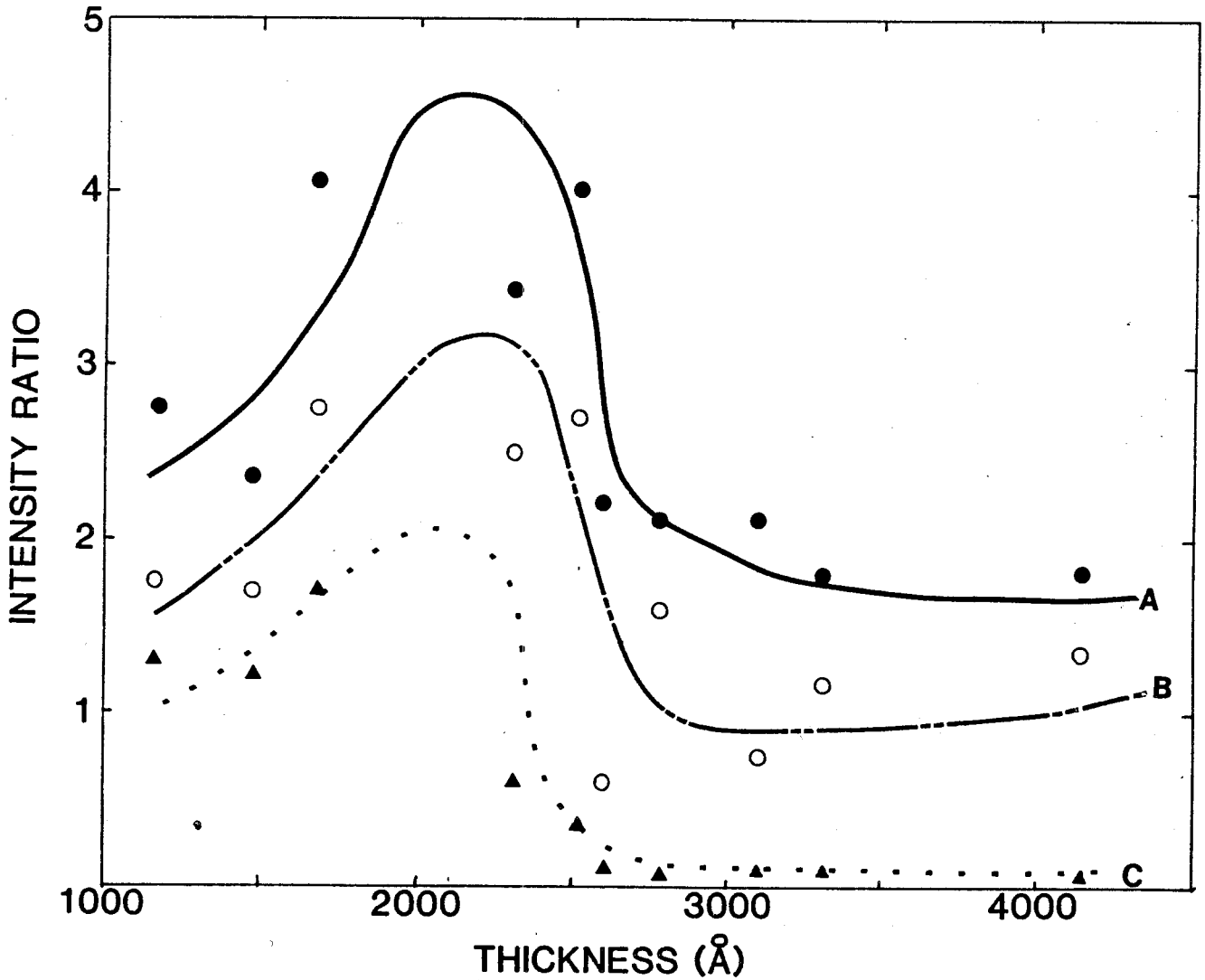
INTENSITY RATIO
5
4
3
2
1
1000
2000
3000
4000
THICKNESS (Å)
A
B
C

Fig.4.11 Dependence of intensity ratio on thickness of the same WO_3 films as in Fig.4.10

● A: [020]/[111]

○ B: [020]/[002]

▲ C: [020]/[001]

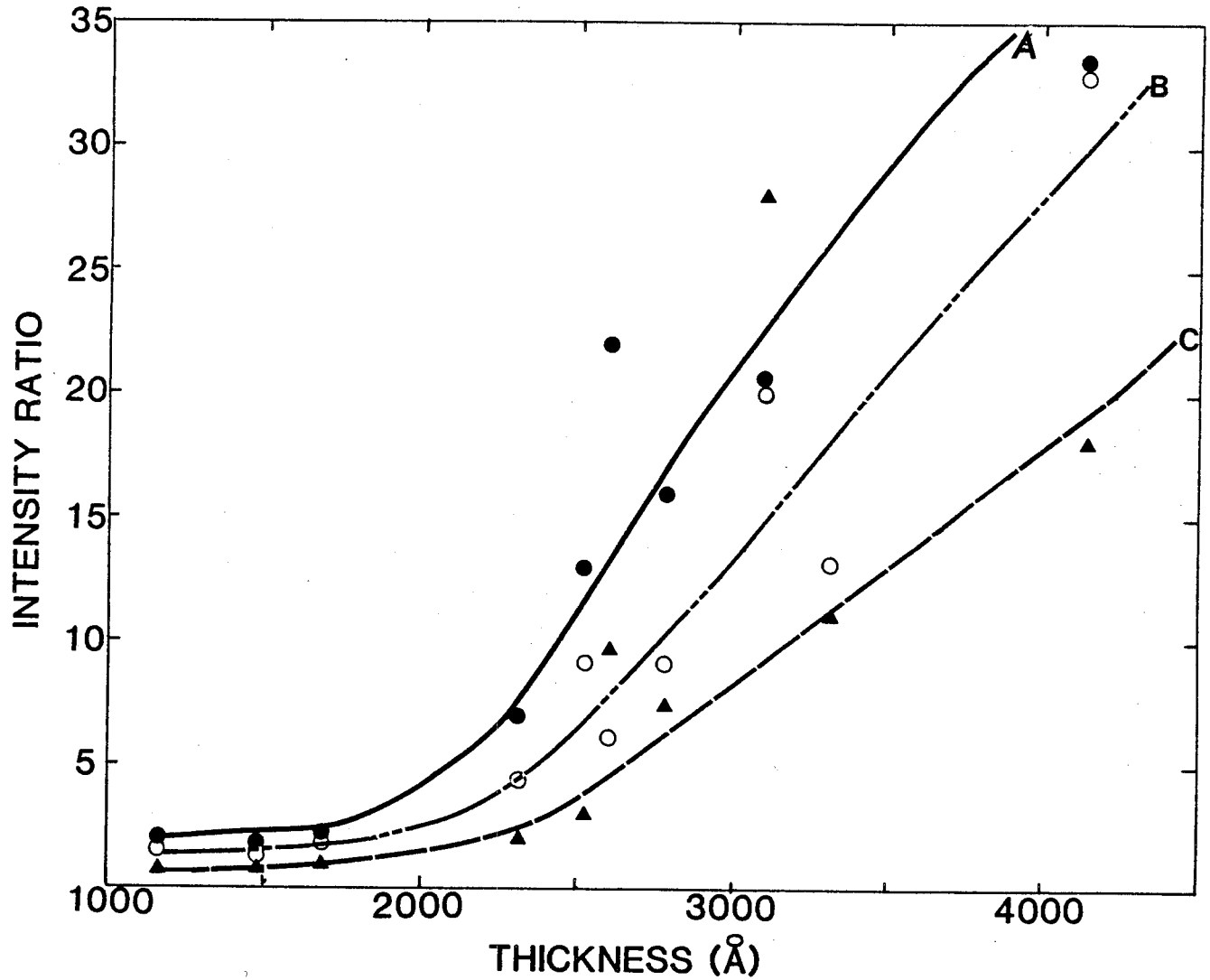
35
30
25
20
15
10
5
INTENSITY RATIO
1000
2000
3000
4000
THICKNESS (Å)
A
B
C

Fig.4.12. Transmittance change at three different wavelengths vs thickness of the same WO_3 films as in Fig.4.11

● A: 9000Å

○ B: 6330Å

▲ C: 5500Å

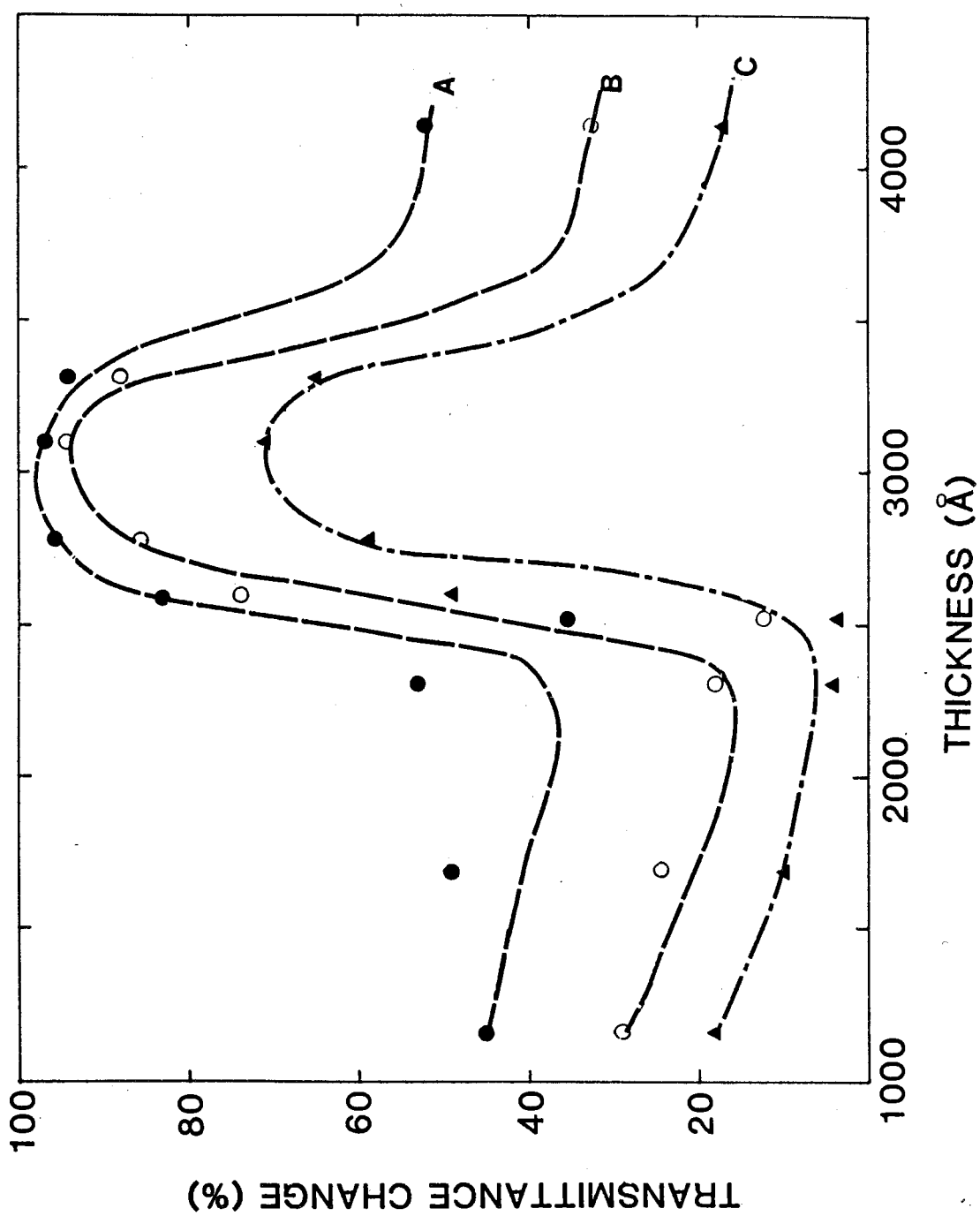
TRANSMITTANCE CHANGE (%)
100
80
60
40
20
1000
2000
3000
4000
THICKNESS (Å)
A
B
C

Fig.4.13 Transmittance change vs crystallite size corresponding to the [001] plane) of four WO_3 films deposited onto polycrystalline SnO_2:F (T_s = 450°C) at substrate temperature of 420°C and N_2 flowrate 16.5 l./min. The film thicknesses were 2550, 2600, 2780 and 3100Å.

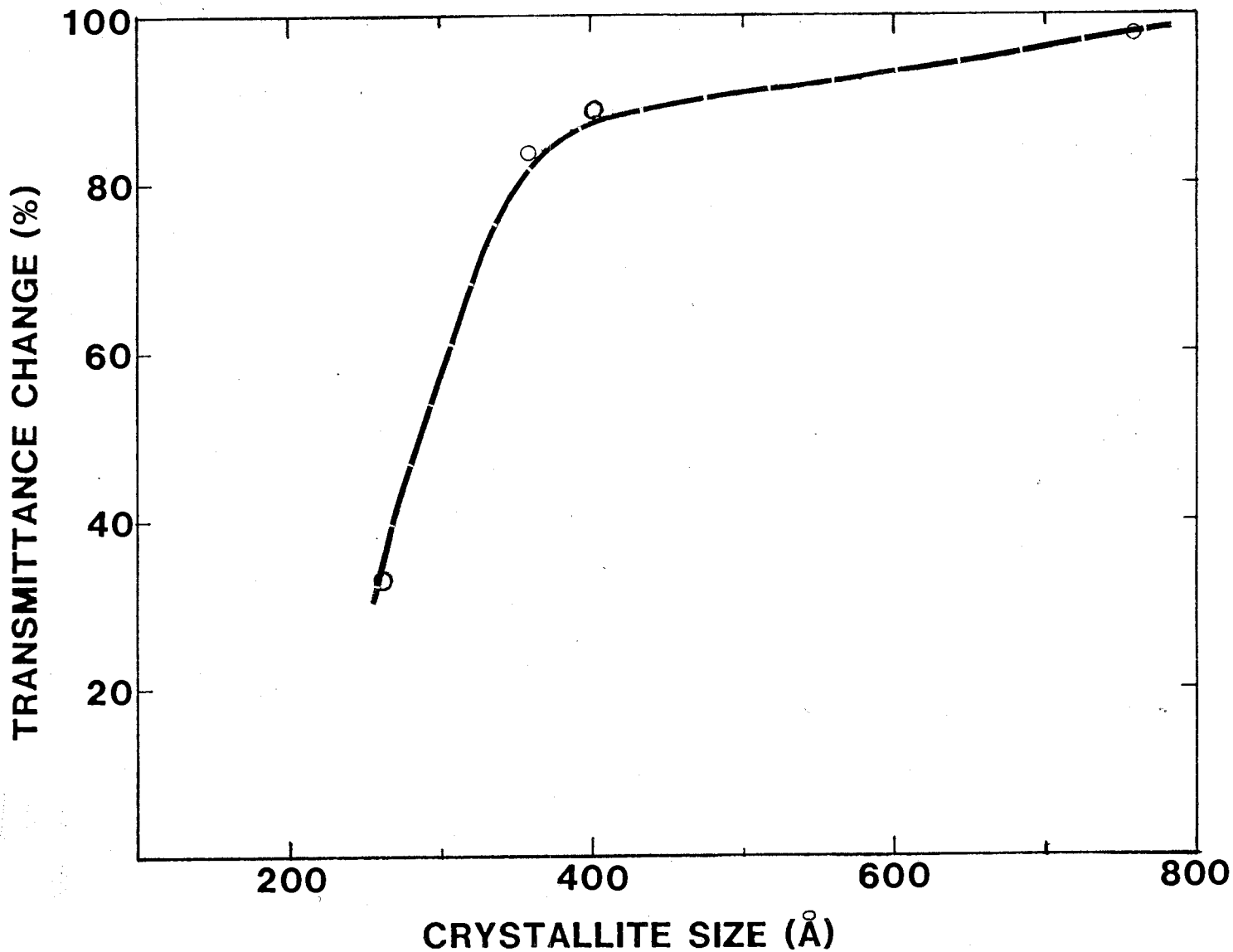
100
80
60
40
20
TRANSMITTANCE CHANGE (%)
200
400
600
800
CRYSTALLITE SIZE (Å)

Fig.4.14 Current--voltage characteristics of a typical experimental ECC

CE: polycrystalline (T_s = 450°C) SnO_2:F film onto glass

WE: WO_3 film of thickness 2780Å on the EC film

RE: Ag/AgCl

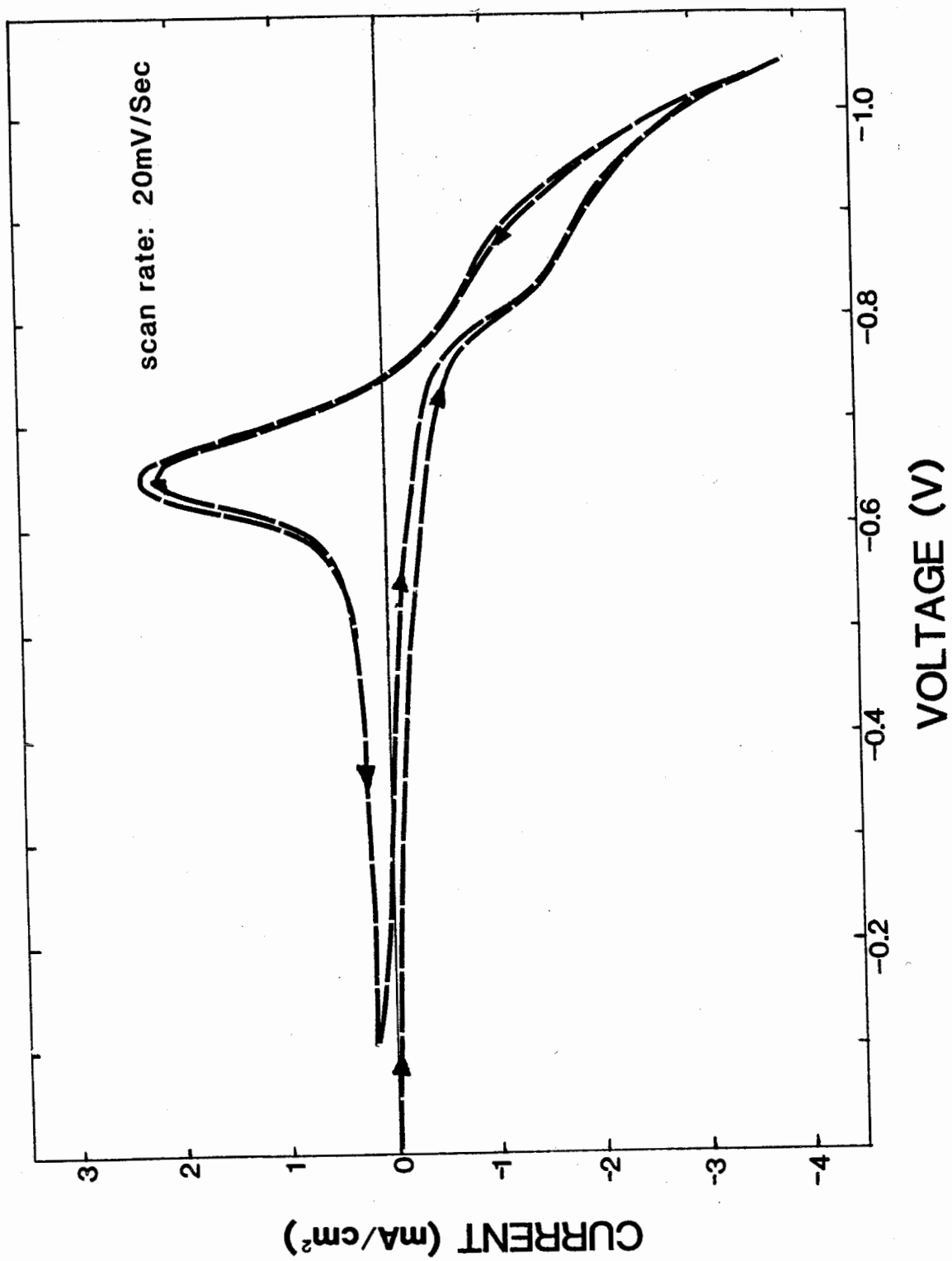
scan rate: 20mV/Sec
CURRENT (mA/cm²)
VOLTAGE (V)
3
2
1
0
-1
-2
-3
-4
-0.2
-0.4
-0.6
-0.8
-1.0

Fig.4.15 Dependence of white light transmittance on applied voltage of the same cell as in Fig.14

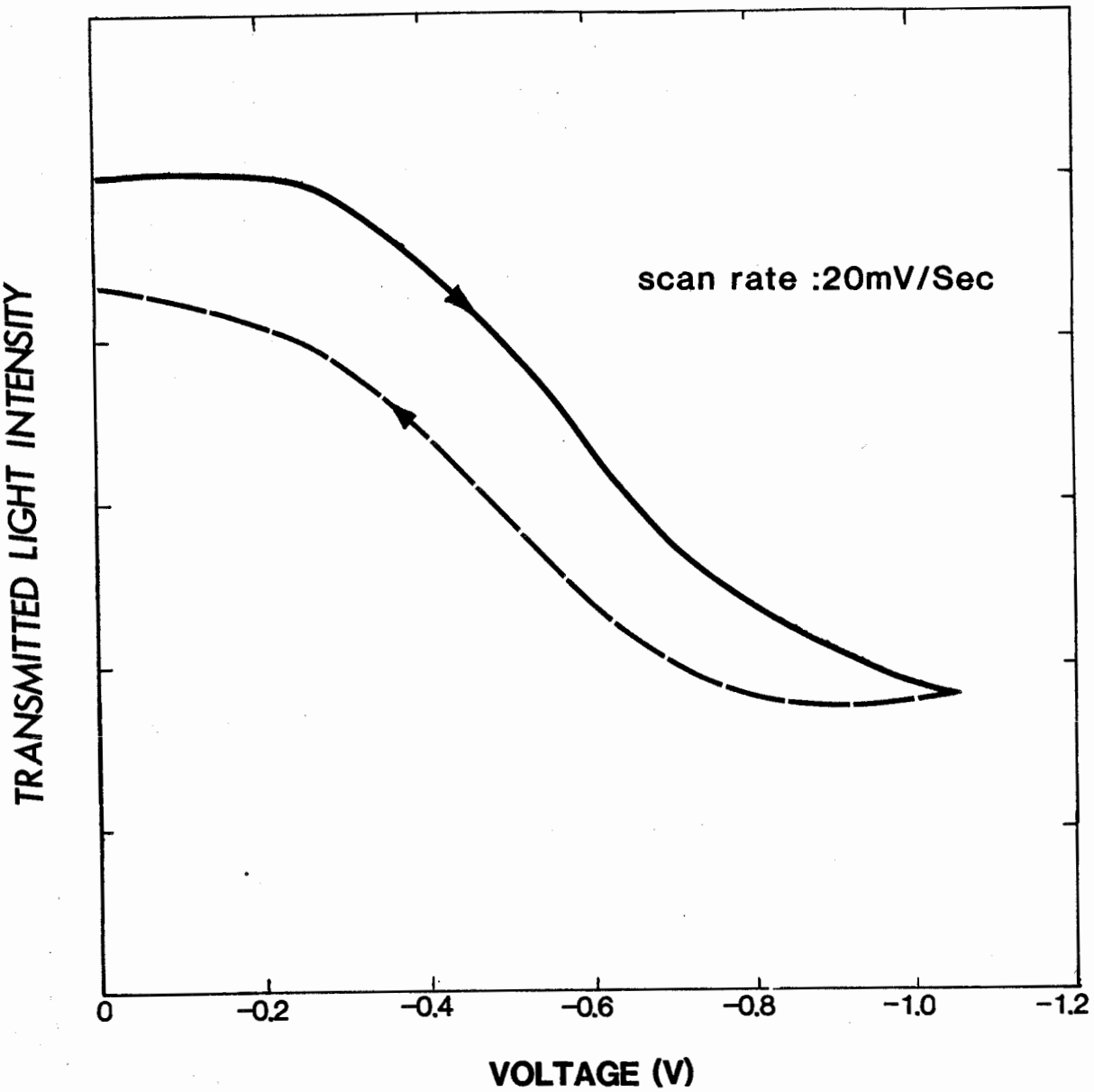
scan rate :20mV/Sec
TRANSMITTED LIGHT INTENSITY
0
-0.2
-0.4
-0.6
-0.8
-1.0
-1.2
VOLTAGE (V)

Fig.4.16 Time response of the same cell as in Fig.4.16

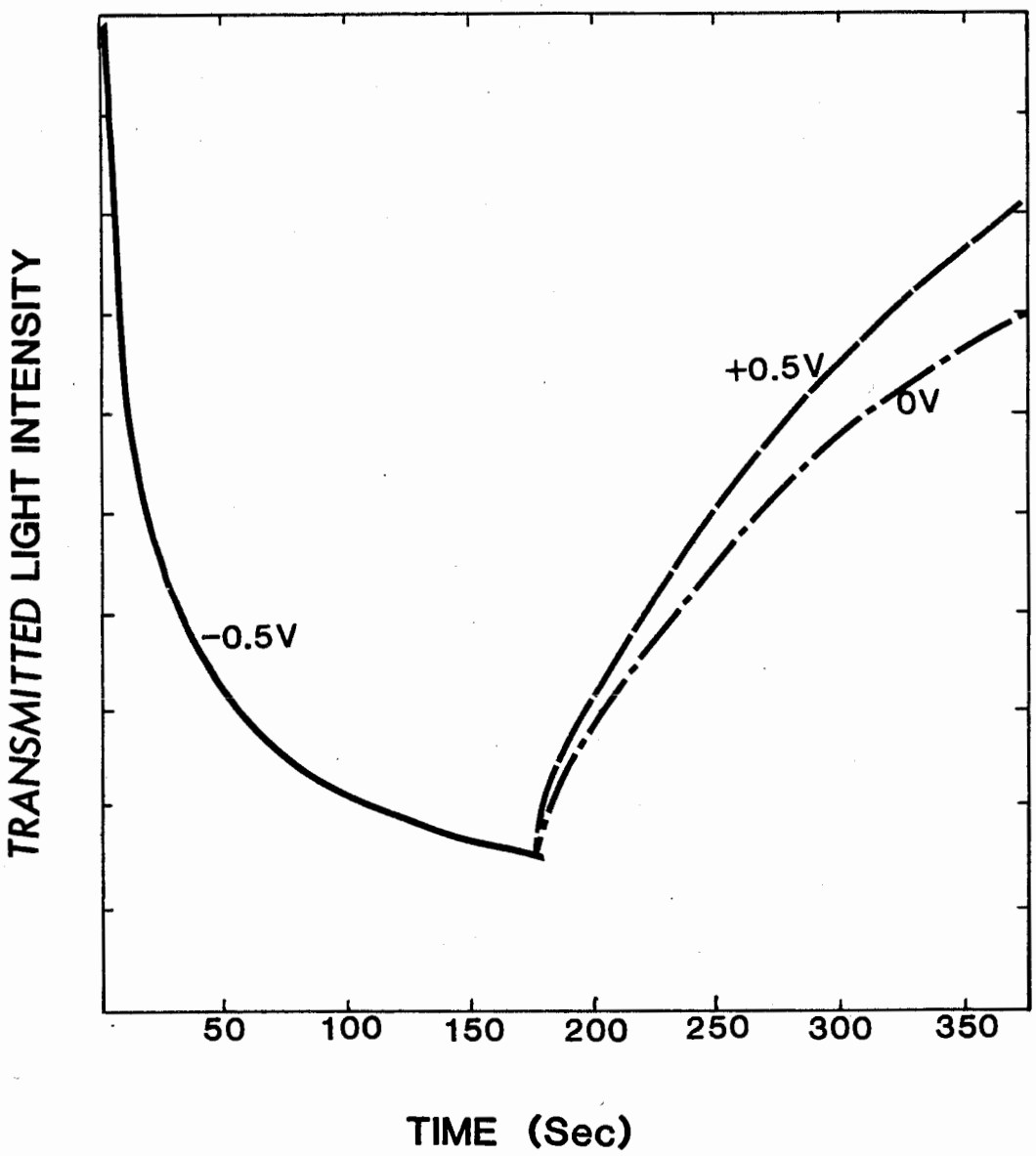
TRANSMITTED LIGHT INTENSITY
-0.5V
+0.5V
0V
50
100
150
200
250
300
350
TIME (Sec)

CHAPTER 5

SUMMARY AND CONCLUSIONS

Pyrolytically spray deposited WO_3 films on SnO_2:F film substrates were investigated.

X-ray diffraction patterns revealed that SnO_2:F films deposited onto glass slides at a substrate temperature of 300°C are amorphous and at substrate temperatures higher than 350°C they are polycrystalline. The degree of the crystallinity of the films is proportional to the substrate temperature during deposition. The amorphous SnO_2:F films are highly resistive with sheet resistances on the order of 10^6 ohms per square (Ω/) and the polycrystalline SnO_2:F films are highly conducting with sheet resistance of 20 to 25 Ω/□. Both amorphous and polycrystalline SnO_2:F films are transparent in the visible light region with an average transmittance of about 80% for polycrystalline films. In order to get highly conducting transparent SnO_2:F films for substrates of WO_3 films, pyrolytically spray deposited SnO_2:F films on glass slides at a substrate temperature of 450°C with a N_2 flowrate of 16.5 l./min for 10 minutes may be the best choice.

WO_3 films were deposited with different deposition

parameters such as the crystalline nature of the substrate, the substrate temperature and the carrier gas flowrate as well as the deposition time. X-ray diffraction studies showed that films of the tungsten chloride solution spray deposited onto the SnO_2:F films at substrate temperatures ranging from 360 to 470°C are polycrystalline with average crystallite sizes ranging from 200 to 800A and mainly tungsten trioxide in composition.

WO_3 films deposited onto polycrystalline (T_s = 450°C) SnO_2:F revealed the largest crystallite size among the four types of SnO_2:F substrate films (amorphous T_s = 300°C; low polycrystalline T_s = 400°C; polycrystalline T_s = 450°C; highly polycrystalline T_s = 500°C) used with other parameters kept constant. This may be due to the nature and smoothness of the substrate surface which influences the atomic mobility and diffusion of tungsten atoms and hence the crystal structure of the WO_3 films. WO_3 films deposited with a N_2 flowrate of 16.5 l./min have the largest crystallite size and a more randomly oriented crystallite orientation among the three value of N_2 flowrate (7.5, 16.5 and 38.0 l./min) used while other parameters were kept constant. This is most likely due to the proper speed of aerosol droplets thereby the proper deposition rate, which affects on the crystal structure of the films. Fixing other parameters except the substrate temperature, WO_3 films deposited onto amorphous SnO_2:F substrate showed an almost constant average crystallite size with an increase in

substrate temperature from 400 to 470°C; WO_3 films deposited onto highly polycrystalline SnO_2:F substrates showed a maximum average crystallite size at a substrate temperature of 420°C, with an increase in substrate temperature from 360 to 470°C during deposition.

X-ray analysis revealed that the thickness of the films did not affect the crystallite size when the film was thicker than 1200Å but the thickness of the films affected the preferential orientation of crystallites. For films deposited onto polycrystalline SnO_2:F substrates, the [001] plane was preferentially oriented for thicknesses from 1200 to 2500Å and the [020] plane was preferentially oriented in thicknesses ranging from 3100 to 4200Å. Thicknesses on the order of 2900Å films showed a slightly [020] preferred orientation but had a more randomly oriented crystallite structure than films with other thicknesses.

The electrochromic performance showed that films which have a larger crystallite size and more randomly oriented crystallite structure showed most remarkable coloration and a near infrared transmittance change of 90%; which most likely results from an increase in reflection. Injected electrons in the film with larger crystallite size show more likely free-electron behavior and in addition less grain boundary scattering, which results in a larger reflection . Films which are more randomly oriented have larger angles of grain boundaries such that more cations and electrons are injected

into the films, which also results in an increased reflection.

The [001] plane preferential orientation of the WO_3 film has a larger influence on the electrochromic behavior than the [020] preferential orientation. This is probably due to the [001] plane corresponding to the lowest surface free energy crystal plane for hexagonal closed-packed (octahedron) crystal thereby the hydrogen diffusion coefficient is the smallest along the $\vec{c}$ crystallographic direction.

Pyrolytically spray deposited tungsten oxide onto polycrystalline (T_s = 450°C) SnO_2:F at a substrate temperature of 420°C and a N_2 flowrate of 16.5 l./min with film thickness about 3000Å, revealed the optimum electrochromic behavior which is desirable for the preparation of " smart windows ".

Bibliography

1. W. B. Fowler, "Physics of Color Centers", Academic Press, New York, p.2 (1968).

2. S. K. Deb, Philos. Mag. 27: 801 (1973).

3. M. Green, Thin Solid Films 50: 145 (1978).

4. R. B. Goldner, D. H. Mendelsohn, J. Alexander, W. R. Henderson, D. Fitzpatrick, T. E. Haas, H. H. Sample, Appl. Phys. Lett. 43: 1093 (1983).

5. R. B. Goldner, Solar Energy Mat. 11: 177 (1984).

6. J. S. E. M. Svensson, C. G. Granqvist, Solar Energy Mat. 12: 391 (1985).

7. J. S. E. M. Svensson, C. G. Granqvist, Thin Solid Films 126: (1985).

8. A.P. Schuster, D. Nguyen, O. Caporaletti, Solar Energy Mat. 13: 153 (1986).

9. B. W. Faughnan, R. S. Crandall, P. M. Heyman, RCA Rev. 36: 177 (1975).

10. K. Miyake, H. Kaneko, M. Sano, N. Suedomi, J. Appl. Phys. 55: 2747 (1984).

11. H.Kaneko, S. Nishimoto, K. Miyake, N. Suedomi, J. appl. Phys. 59: 2526 (1986).

12. A. Chemseddine, R. Morineau, J. Livage, Solid State Ionics 9: 357 (1983).

13. C. E. Tracy, D. K. Benson, J. Vac. Sci. Technol. A4: 2377 (1986).

14. D. Craigen, A. Mackintosh, J. Hickman, K. Colbow, J. Electrochem. Soc. 133: 1529 (1986).

15. J. E. S. M. Svensson, C. G. Granqvist, Appl. Phys. Lett. 45: 828 (1984).

16. O. F. Schirmer, V. Wittwer, G. Baur, G. Brandt, J. Electrochem. Soc. 124: 797 (1977).

17. D. W. Bullett, J. Phys. C:Solid State Phys. 16: 2197 (1983).

18. C. M. Lampert, Solar Energy Mat. 11: 1 (1984).

19. R. J. Colton, J. Appl. Phys. 49: 409 (1978)

20. E. K. Sichel, J. I. Gittleman, J. Zelez, Appl. Phys. Lett. 31: 109 (1977).

21. R. B. Goldner, P. Norton, K. Wong, G. Foley, E.L. Goldner, G. Seward, R. Chapmam, Appl. Phys. Lett. 47: 536 (1985).

22. E. Salje, K. Viswanathan, Acta Cryst. A31: 356 (1975)

23. K. Kopp, B. N. Harmon, S. H. Liu, Solid State Commun. 22: 677 (1977).

24. F. P. Koffyberg, K. Dwight, A. Wold, Solid State Commun. 30: 433 (1979).

25. S. Tanisaki, J. Phys. Soc. Japan. 15: 566 (1960).

26. S. Tanisaki, J. Phys. Soc. Japan. 15: 573 (1960).

27. B. O. Loopstra, H. M. Rietveld, Acta Cryst. B25: 1420 (1969).

28. E. Salje, Acta Cryst. B33: 574 (1977).

29. J. V. Gabrusenoks, P. D. Cikmach, A. R. Lusis, J. J. Kleperis, G. M. Ramans, Solid State Ionics 14: 25 (1984).

30. P. G. Dickens, R. M. P. Quilliam, M. S. Whittingham, Mat. Res. Bull. 3: 941 (1968).

31. P. J. Wisenman, P. G. Dickens, J. Solid State Chem. 6: 374 (1973).

32. I. F. Chang, B. L. Gilbert, T. I. Sun, J. Electrochem. Soc. 122: 955 (1975).

33. R. Hurditch, Electron Lett. 11: 142 (1975).

34. B. W. Faughnan, R. Crandall, Appl. Phys. Lett. 31: 834 (1977).

35. T. Nishimura, K. Taira, S. Kurita, Appl. Phys. Lett. 36: 585 (1980).

36. P. G. Dickens, S. J. Hibble, S. A. Kay, M. A. Steers, Solid State Ionics 20: 209 (1986).

37. R. S. Crandall, P. J. Wojtowicz, B. W. Faughnan, Solid State Commun. 18: 1409 (1976).

38. H. Muramatsu, T. Itoh, A. Watanabe, K. Hara, Jap. J. Appl. Phys. 21: 73 (1982).

39. W. C. Dautremont-Smith, M. Green, K. S. Kang, Electrochem. Acta 22: 751 (1977).

40. N. F. Mott, "Metal-Insulator Transitions", Taylor and Francis, London, p.124 (1974).

41. G. D. Mahan, "Many-Particle Physics", Plenum Press, New York, p.385 (1981).

42. S. F. Cogan, T. D. Plante, M. A. Parker, R. D. Rauh, J. Appl. Phys. 60: 2735 (1986).

43. L. I. Mirkin, "Handbook of X-ray Analysis of Polycrystalline Materials", Consultants Bureau, New York, (1964).

44. E. W. Nuffield, "X-Ray Diffraction Methods", John Wiley and Sons, New York, p.147 (1966).

45. M. N. Islam, M. O. Hakim, J. Phys. Chem. Solids 46: 339 (1985).

46. T. Arai, J. Phys. Soc. Japan, 15: 916 (1960).

47. M. Fantini, I. L. Torriani, C. Constantino, J. Crystal Growth 74: 439 (1986).

48. K. L. Chopra, "Thin Film Phenomena", McGraw-Hill Book Company, New York, (1969).

49. J. S. Maudes, T.Rodriguez, Thin Solid Films 69: 183 (1980).

50. B. S. Acharya, L. D. Pradhan, J. Appl. Cryst. 19: (1986).

51. J. M. Poate, K. N. Tu, J. W. Mayer, "Thin Films-Interdiffusion and Reaction", John Wiley and Sons, New York, p.88 (1978).

52. S. K. Joo, I. D. Raistrick, R. A. Huggins, Solid State Ionics 17: 313 (1985).

53. R. B. Goldner, A. Brofos, G. Foley, E. L. Goldner, T. E. Haas, W. Henderson, P. Norton, B. A. Ratnam, N. Weis, K. K. Wong, Solar Energy Mat. 12: 403 (1985).

54. N. Yoshiike, S. Kondo, J. Electrochem. Soc. 131: 809 (1984).

55. T. Yoshimura, M. Watanabe, Y. Koike, K. Kiyota, M. Tanaka, Jpn. J Appl.Phys. 22: 152 (1983).